UNITED STATES ATOMIC ENERGY COMMISSION

ISC-119

NUCLEAR DISINTEGRATION STUDIES WITH A BETA-RAY SPECTROMETER

By
William W. Pratt

August 1950

Ames Laboratory

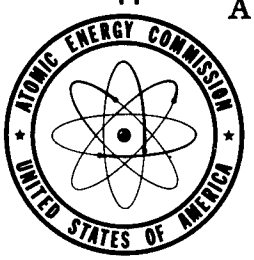

Technical Information Service, Oak Ridge, Tennessee

PHYSICS

Reproduced direct from copy
as submitted to this office.

Work performed under
Contract No. W-7405-eng-82.

PRINTED IN USA
PRICE 35 CENTS

AEC, Oak Ridge, Tenn., 4-12-51—865-W3283

NUCLEAR DISINTEGRATION STUDIES WITH A BETA-RAY SPECTROMETER[1]

by

William W. Pratt

I. ABSTRACT

The use of a beta-ray spectrometer, in the analysis of nuclear decay schemes, makes possible the solution of many of the problems which arise in the course of such analyses. Of particular interest is the application of the instrument to the determination of the energy of beta- and gamma-radiation from radioactive isotopes. In addition, it is possible to use the instrument to estimate the relative intensities of the various components of radiation; and to apply the coincidence method, in conjunction with the spectrometer, to the determination of the order in which these components are emitted from the nucleus.

The present work was concerned with three particular problems arising in beta-ray spectrometry.

A method of improving the intensity-resolution relationship of a thin lens magnetic beta-ray spectrometer, by means of ring focusing, was investigated. The existence of a ring- shaped constriction in the electron beam was demonstrated experimentally by a photographic film method. Making use of the photographic mapping of the beam, an annular baffle was designed. Optimum relations between annular width, solid angle and counter window diameter were investigated. A comparison of this type of baffle system with the original baffle system showed that at 2.5 per cent resolution the spectrometer transmission may be increased by a factor of two by the use of an annular aperture in the region of beam constriction.

---

[1]Doctoral thesis number 1099, submitted August 18, 1950. Work done under the direction of L. J. Laslett.

A theoretical analysis was carried out in an attempt to determine relations from which the relative intensities of beta-rays, gamma-rays and internal conversion electrons might be determined from data obtained with the spectrometer. Simplifying assumptions were made concerning the focusing action of the instrument, and effects due to scattering of electrons in the source of photoelectric radiator were neglected. Formulae were derived from which the observed spectrometer counting rates due to sources of known activity, emitting beta-rays, gamma-rays or internal conversion electrons may be predicted.

The results may be expressed in terms of a quantity defined as the spectrometer efficiency e_s. If internal conversion electrons are being counted, e_s is defined as the ratio of spectrometer counting rate at the peak of the spectral line to the rate of emission of internal conversion electrons by the source. If beta-rays are being counted, e_s is defined as the ratio of spectrometer counting rate at any arbitrary value of the focusing current to the rate of emission of beta-rays by the source. The efficiency in this case will thus be a function of the focusing current. If gamma-rays are being counted by the detection of photoelectrons emitted from a radiating foil, e_s is defined as the ratio of spectrometer counting rate at the peak of the spectral line to the rate of emission by the source of the gamma-quanta concerned.

The results for these three cases are:

$$e_s \text{ (internal conversion electrons)} = e_o S(\alpha),$$

$$e_s \text{ (beta-rays)} = e_o \, h \, p_o \, n(p_o) \, / \, N,$$

$$e_s \text{ (gamma-rays)} = e_o \, S(\alpha) \, \tau \quad X.$$

The notation used is as follows: The quantity e_o is the efficiency of the spectrometer for counting monoenergetic electrons and is thus the product of the fractional solid angle collected and of the intrinsic efficiency of the spectrometer counter. $S(\alpha)$ is a function of the parameter α given by

$$S(\alpha) = (1 - \alpha/2) \text{ for } \alpha < 1 \; ;$$

$$S(\alpha) = 1/(2\alpha) \text{ for } \alpha > 1 \; .$$

The parameter α is the ratio of the momentum loss of an electron of momentum p_o in traversing the source of photoelectric radiator to the base of the spectrometer transmission curve, where p_o, the focused momentum, is the momentum of the electrons selected by the spectrometer baffle system. The quantity h is the fractional half-width ($\delta p/p_o$) of the transmission curve. The function $n(p_o)$ is the rate of emission of beta-particles per unit momentum interval, and N is the total rate of emission of beta-particles by the source. The factor τ is the photoelectric absorption coefficient of the radiator for the orbital shell concerned, and X is the thickness of the photoelectron radiator.

Due to the assumptions made, the accuracy of these formulae is such that they furnish an estimate only. It is suggested, however, that they may be treated as semi-empirical relations by means of which data may be reliably interpolated.

The application of the spectrometer to the methods of coincidence counting has been considered. Statistical considerations may be used to predict the limitations of the spectrometer with respect to the types of coincidence measurements which may be carried out successfully. The methods of coincidence spectrometry were applied to an analysis of the decay scheme of Hf^{181}. Both electron-electron and gamma-electron coincidences were investigated. The efficiency of the gamma-counter used was determined by coincidence methods, using the known decay schemes of Co^{60} and ThB.

The result of the measurements indicated delayed coincidences between the beta particles and the gamma-ray transitions of 130 Kev and 471 Kev energy.* They also indicated non-delayed coincidences between the 130 Kev and 471 Kev gamma-ray transitions. The part of the Hf^{181} decay scheme involving these transitions, proposed by Chu and Wiedenbeck,* is thus confirmed by these measurements. The results do not serve to distinguish between the complete decay scheme of Chu and Wiedenbeck and modifications such as that proposed by Deutsch and Hedgran**.

---

*Chu, K. Y. and Wiedenbeck, M. L. The Radiations from Hf^{181}. Physical Review. 75:226-231. 1949.

**Deutsch, M. and Hedgran, A. Radioactivity of Hf^{181}. Physical Review. 79:400-401. 1950.

II. INTRODUCTION

The use of the beta-ray spectrometer, in the analysis of nuclear decay schemes, has been discussed by several authors (1-3). The primary use of the instrument consists in the determination of energies of beta-rays, internal conversion electrons, and of gamma-radiation through the analysis of the secondary electrons produced in a radiating foil. In addition to the determination of energy, which is discussed in detail in references 1-3, it is possible to estimate the relative intensities of the various types of radiation studied. A further extension of the application of the spectrometer consists in the introduction of a secondary detector of radiation, and of the measurement of coincidences between the electrons selected by the spectrometer and the radiations detected by the secondary detector. The three types of measurement mentioned above, if carried out with sufficient precision, permit the decay scheme of the radioactive isotope under consideration to be determined. The work reported here will be concerned with three particular features of the application of the spectrometer to the determination of nuclear decay schemes. The instrument described in this work is a magnetic focusing spectrometer of the thin lens type. Its construction features have been described in detail by Jensen (3). In section IV a method of improving the performance of the instrument, through the use of a new type of baffle system, will be described. In section V the possibilities and limitations of the determination of relative intensities will be considered. In section VI the application of the spectrometer to the method of coincidence counting will be described.

III. REVIEW OF THE LITERATURE

The principles involved in the use of the magnetic lens spectrometer for the determination of electron energies have been discussed in detail in references 1-3. It is shown in these references that, through the use of an appropriate baffle system, and a suitable magnetic field, electrons with momenta in a small range of the order of 1-2% may be selected and "focused" on the aperture of a Geiger counter, or other suitable detector. Electrons of other momenta are caused to strike one of the baffles, and are thus prevented from reaching the counter. Both Siegbahn (1) and Deutsch, Elliott and Evans (2) have considered the relation between resolution of the instrument and transmitted electron

intensity. Jensen (3) has considered the effect of the momentum loss in the source on the determination of the electron energy from the observed focusing current. Deutsch, Elliott and Evans (2) have proposed a semi-empirical method for the determination of the relative intensities of gamma-rays.

The existence of ring focusing (section IV) in spectrometers of the solenoid type was first proposed by Witcher (4). Recently it was suggested by Frankel (5) that this type of focusing may also exist in spectrometers of the thin lens type. This problem has been considered theoretically by Keller, Koenigsberg and Paskin (6,7). They predicted an increase by a factor of two in intensity, for a given resolution, through the use of ring focusing. Verster (8) has considered the same problem both theoretically and experimentally, and has arrived at similar conclusions.

The application of coincidence counting in the analysis of nuclear decay schemes has been treated in a general way by Mitchell (9), who has considered in particular the use of absorbers to discriminate against electrons and quanta of different energies. Dunworth (10) has considered a possible approach to the statistical problems involved in conducting a coincidence experiment. Roberts and others (11-16) have described coincidence experiments in the study of several particular decay schemes, and have indicated how it is possible to determine counter efficiencies experimentally in the process of making such studies. Coincidence measurements in the spectrometer are discussed by Norling (17), and by Siegbahn and Johansson (18). Norling (17) has treated in considerable detail the problems of counting losses due to dead time of counters and associated circuits, of methods of testing counters and circuits, and of the theoretical determination of the efficiencies of gamma-counters. Siegbahn and Johansson (18) have determined several decay schemes by the method of coincidence spectrometry. Recently Feather, Kyles and Pringle (19) have indicated how it is possible to use a spectrometer which will simultaneously select electrons in two energy groups. It is possible, by counting coincidences between these two groups, to determine with certainty which radiations occur in cascade transitions.

Further work by other authors will be cited in the body of this report.

IV. RING FOCUSING

A. Introduction

The existence of ring focusing in spectrometers of the magnetic lens type has been discussed by various authors (4-8, 20-23). In all cases so far investigated it appears that a ring-shaped constriction exists in the electron beam in a plane between the source and counter. Thus it is found that by designing a baffle system such that a narrow annular aperture is presented to the beam in the region of constriction, an improvement in focusing characteristics may be obtained over the so-called axial focusing case in which a counter window on the axis is used as the discriminating aperture. It was the purpose of this investigation to determine experimentally the position of the constriction in the beam and to determine the improvement in focusing obtained by the use of an annular aperture at this position.

B. Location of Ring Focusing

The instrument used in this investigation (reference 3) has a 25 cm focal length; and the distance between the source and its image on the axis is 100 cm; so that the coil is midway between the source and its image. The half-width of the magnetic field is 13.6 cm. The baffle system originally used for axial focusing is shown in Fig. 1. The baffles A and B select electrons emitted from the source in a solid angle Ω, and these electrons are focused on the counter by the magnetic field. The counter window diameter is made equal to the diameter of the electron beam. To observe the existence of ring focusing, photographic films were placed in the spectrometer in a plane perpendicular to the axis, as shown by the dotted line C in Fig. 1. The baffle A was removed, and reinserted at the source end of the spectrometer, as shown by the dotted lines A'. The baffle D, which does not come in contact with the focused electron beam, but is for the purpose of eliminating scattering, was removed. The electron beam, defined by the trajectories a and b, was then limited by the baffles A' and B. A thin source of Cs^{137} was inserted at the source end of the spectrometer, and the coil current necessary to focus the K internal conversion line of the 0.66 Mev gamma-ray on an 0.82 cm diameter counter aperture was determined. The film C was

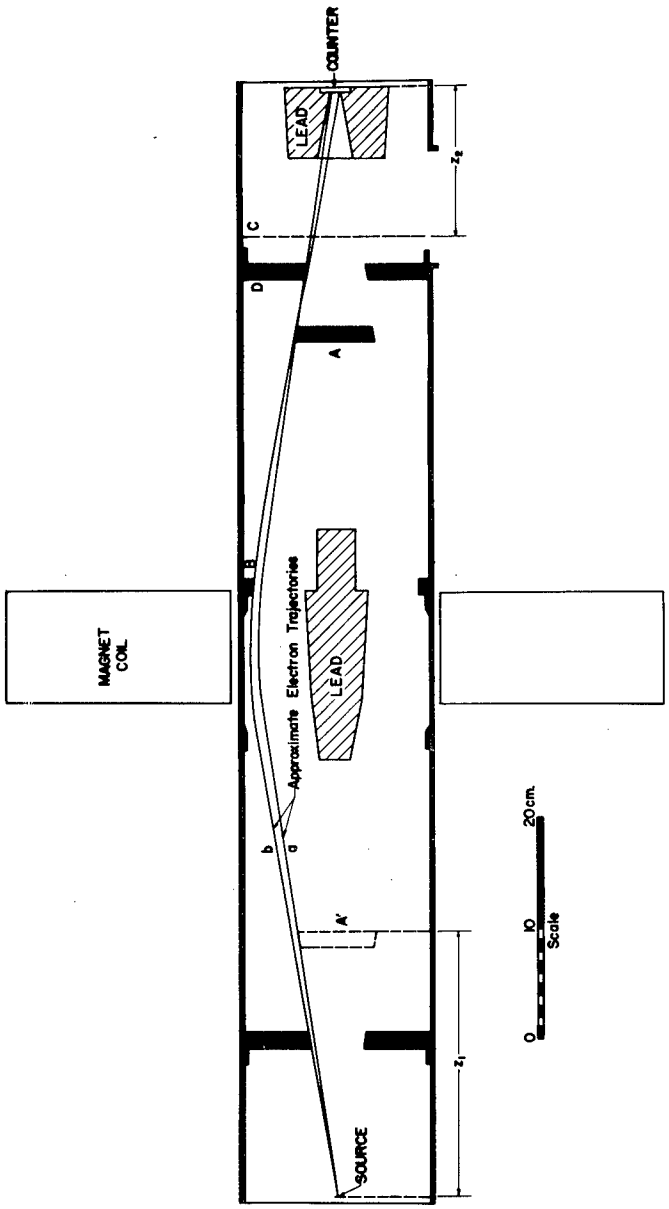

Fig. 1--Spectrometer baffle system for axial focusing.

then placed in position and exposed for 19 hours, with the above determined current through the coil. Exposures were made with films at various distances Z_2 from the counter plane. It was found that with $Z_2 \approx 20$ cm a ring image, corresponding to the focused K line, was obtained which was narrower than the images for Z_2 greater or less than 20 cm. It is estimated that the position Z_2 corresponding to the narrowest ring can be found by this method to within $\pm$ 2 cm. The ring obtained at 20 cm is shown in Fig. 2, which also shows a ring of larger diameter corresponding to the higher energy L line. The inner and outer diameters of the K ring are 5.2 cm and 6.1 cm respectively. In this experiment Z_1 (Fig. 1) was taken as 30.27 cm, which was estimated to correspond to the same solid angle as had been used in most of the previous work with axial focusing.

C. Baffle Design

After thus locating the position, mean diameter, and width of the narrowest part of the focused electron beam, a baffle system was constructed to make use of this constriction in the beam. The baffle system used for ring focusing is shown in Fig. 3. The fixed baffle C' has a central circular aperture of mean diameter 6.10 cm. The plane of the center of this baffle is placed 20 cm from the plane of the counter window. The movable baffle C also has a mean diameter of 6.10 cm, and is attached to an 0.25 inch rod, extending through the end of the spectrometer tube, by means of which the baffle may be adjusted axially along the tube. Similarly, baffle A' may be adjusted axially along the tube to limit the electron solid angle.

With this system of baffles it is possible to vary the location of A' and C as well as the counter window diameter, and in this way to vary the resolution of the instrument, and simultaneously the accepted solid angle. It is of course desirable to determine the optimum relation between the variable parameters, so that for a given resolution the largest possible solid angle may be obtained. This was done in the work described here by determining a large number of line shape curves with the spectrometer, corresponding to various combinations of the three variable parameters.

Before considering the results of these measurements, it will be of interest to consider two problems concerning the design and insertion of the ring baffles C and C'.

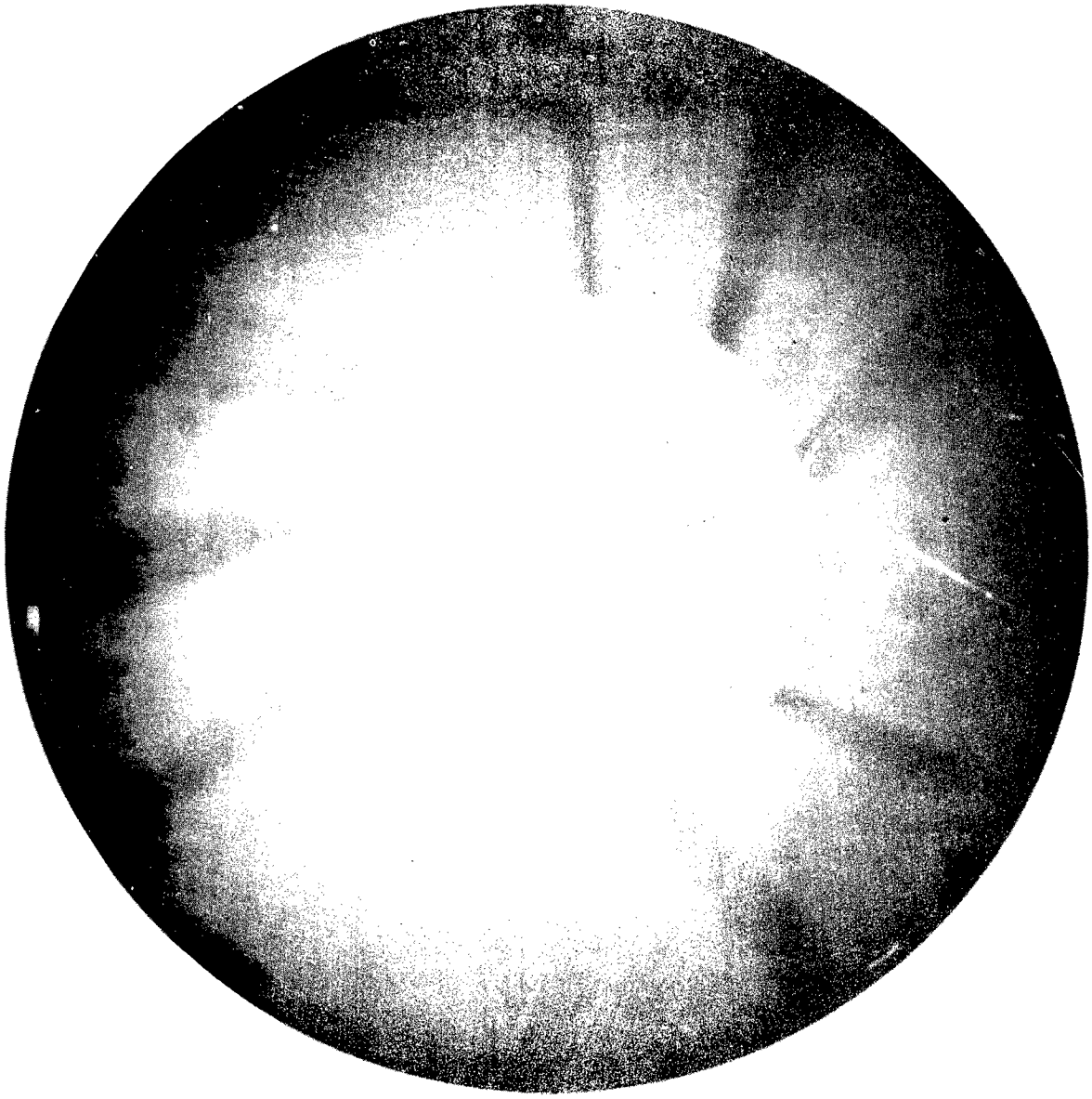

Fig. 2--Photographic image of electron beam from Cs^{137} source.

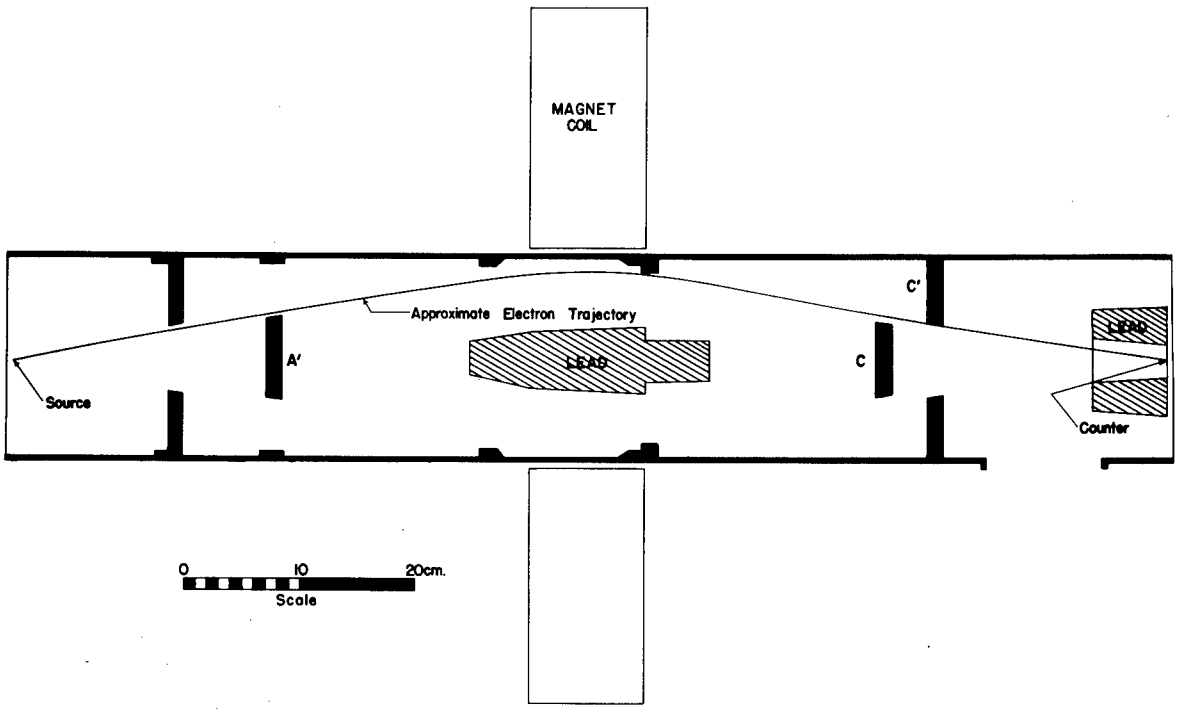

Fig. 3--Spectrometer baffle system for ring focusing.

The orbit calculations made by the theoretical group in this laboratory (7), which were completed before this baffle was designed, showed that in the plane of constriction of the beam the trajectory with the largest diameter corresponds to a particular angle of emergence of the electrons from the source with respect to the spectrometer axis. This angle is found to be approximately 8.5°. Since, in making the photographic record of the trajectories, the angles selected by the baffles A' and B were 7° and 10° respectively, this trajectory of greatest ring diameter was included in the photographic image. Thus the baffle C', with a diameter equal to the outer diameter of the photographic ring image, will not cut out part of the beam regardless of the setting of the solid angle baffle A'. It will, in fact, coincide with the outer edge of the beam whenever baffle A' subtends an angle at the source less than 8.5°.

Due to the small width of the electron beam in the region of constriction, and the consequently narrow annulus used between baffles C and C', it will be recognized that the alignment of C and C' with respect to the spectrometer axis is critical. If these baffles are not located centrally with respect to the spectrometer axis, then mono-energetic electrons, emitted at different azimuthal angles, will require different focusing currents. This will result in an increase in the half-width of the spectral line. In order to align these baffles properly they were constructed on a common assembly which could be inserted into the spectrometer as a single unit. After inserting this unit, four line shape curves were obtained, using the photoelectron line from K conversion in lead due to the 1.3 Mev gamma-ray of Co^{60}. For each line shape curve, electrons entering only one quadrant of the focusing region were used; the other three quadrants were masked out by the use of a sector baffle inserted for this particular experiment. This baffle was made of a disc of 1.27 cm micarta with one quadrant cut out, and was inserted in a plane perpendicular to the spectrometer axis at a distance of 12.8 cm from the source. A failure to align the ring baffles C and C' in the center of the spectrometer will cause the spectral lines obtained with different aximuthal orientations of the sector baffle to occur at different values of coil current. The magnitude of this effect may be estimated by the use of the thin lens formula (reference 2). The result is

$$\frac{\delta I}{I} = \frac{be}{a(2f-b)}$$

where $\delta I/I$ is the fractional shift in the peak with opposite sectors open, a is the mean diameter of the ring baffles, b is the distance from the ring baffles to the counter position, f is the focal length of the magnetic lens, and e is the amount by which the center of the ring baffle is displaced from the spectrometer axis. In the present case, b = 20 cm, a = 6.1 cm and f = 25 cm. Thus

$$e = 9.15 \quad \delta I/I \text{ cm} .$$

The limit of detection of $\delta I/I$ is of the order of 0.2%, so that values of e of 0.2 mm may be detected. The widening of the half-width h of the spectral line, due to baffle misalignment, is estimated to be $\delta h = 1/2 \ \delta I/I$. In the present case, with $\delta I/I = 0.2\%$, this results in $\delta h = 0.1\%$. Fig. 4 shows peaks obtained before and after radial alignment of the ring baffle. It is seen that the relative displacement of the peaks has been reduced to about 0.2% and thus it is estimated that the contribution to the half-width of the spectral line is of the order of 0.1%.

D. Experimental Results

When the ring baffles had been adjusted with their centers on the spectrometer axis, 50 line shape curves were determined, using the monoenergetic electrons from the internal conversion F line of ThB. These curves correspond to different settings of the three parameters; baffle A' position, baffle C position and counter aperture diameter W. A source diameter of 0.5 cm was used throughout. It will be of more direct interest to express the position of baffle A' in terms of the solid angle Ω subtended by the limiting orbits a and b (Fig. 1), as determined by the calculations (reference 7). It will also be desirable to express the position of baffle C in terms of an effective ring width R, defined by $R = S(Z-20)$. The mean slope S of the trajectories in the vicinity of the ring baffles has been determined by the calculations (reference 7) to be about 0.15. Z is the distance in cm between the center of baffle C and the counter aperture.

Fig 5 shows the results obtained using a counter with a 2.7 cm diameter aperture, which was the largest counter aperture available. The half-width of the spectral line is plotted as a function of the maximum counting rate at the peak of the line shape curve. The intensity is plotted on an

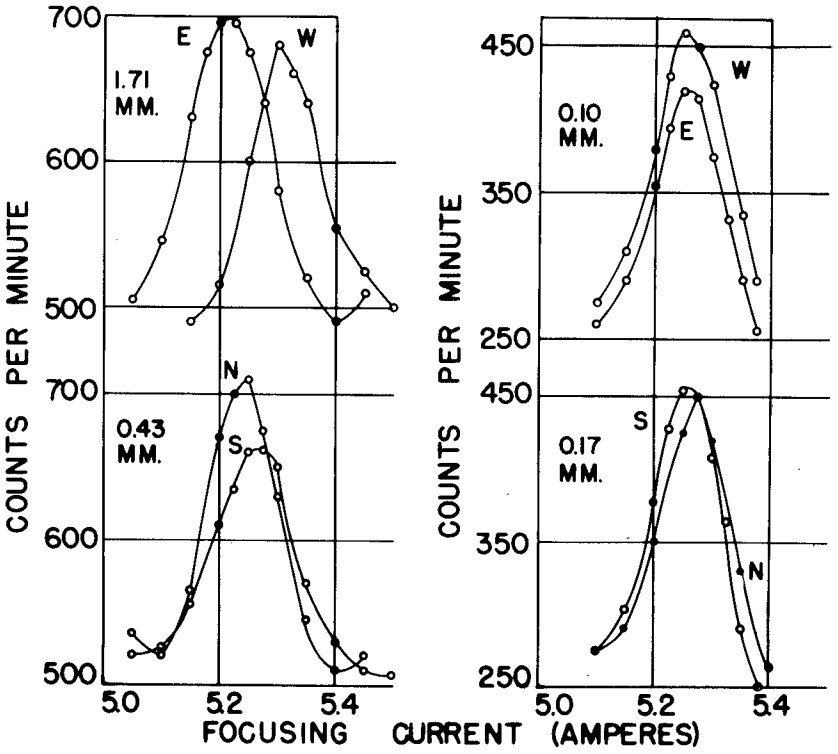

Fig. 4--Ring baffle alignment test. Peaks at the left were taken before centering the baffle and peaks at the right were taken after centering the baffle. The open sector is indicated for each peak by the letters N, S, E, and W. The amount by which the baffle is estimated to be off center is indicated by the numbers beside each pair of peaks.

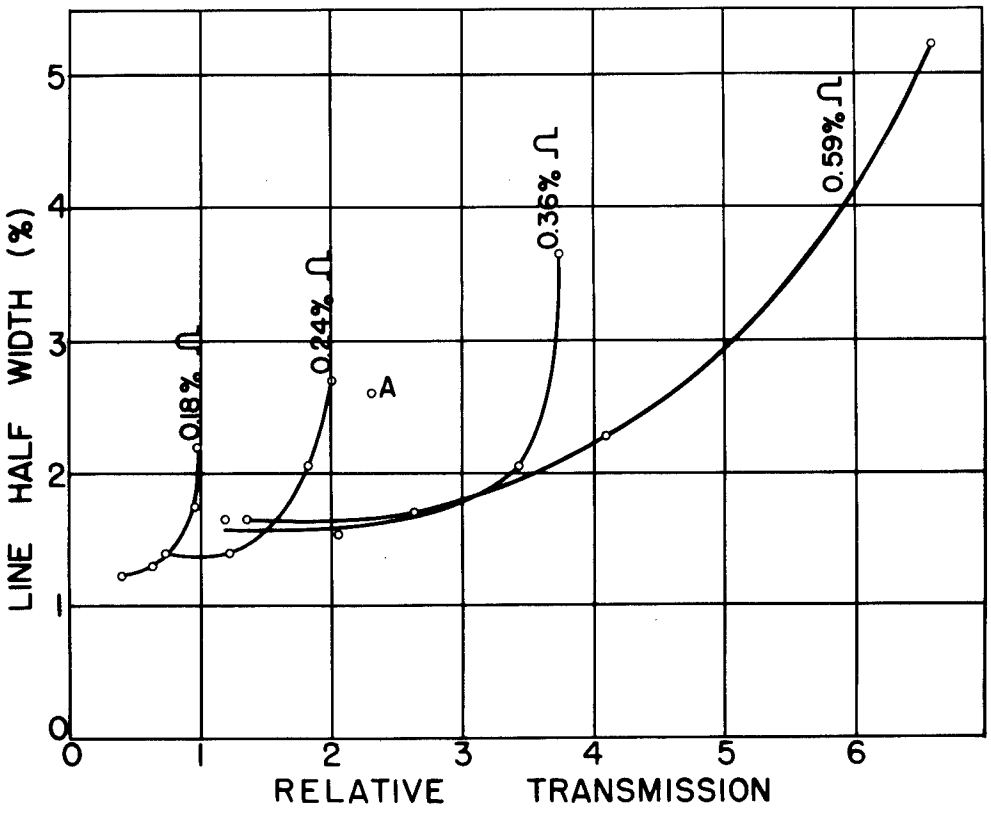

Fig. 5--Transmission-resolution relation as a function of solid angle and ring width. The point A represents an axial focusing case.

arbitrary scale, and includes corrections for source decay and for the relative strengths of the several ThB sources used. For each curve in Fig. 5 the intensity is varied by varying the ring width R. Each curve is for a different solid angle Ω measured in per cent of 4π. It is seen from Fig. 5 that for a given half-width the maximum intensity is obtained by a proper choice of both Ω and R. Thus the optimum operating curve is determined by the envelope of the curves in Fig. 5; and the parameters Ω and R are uniquely related to the desired half-width by this envelope. It is seen, however, that the 0.59% solid angle setting gives results which differ very little from the optimum conditions, for half-widths greater than about 1.6%. Since for half-widths below 1.6% a transmitted intensity is obtained which is usually too low to be of interest, in practice it is found convenient to leave the solid angle baffle A' fixed and to select the desired resolution by varying only the ring width R. It is evident from Fig. 5 that a larger solid angle than 0.59% would be expected to give somewhat better intensity at half-widths of the order of 2% or greater. However, since some further modifications of the instrument would be required to achieve this increased solid angle, and since in any event the improvement obtained would not be expected to be very great, this has not as yet been done.

Line shape curves using other counter aperture diameters showed the same general features as those represented in Fig. 5. In each case the solid angle setting of 0.59% gave the best intensity for a given half-width, except in the region of excessively low intensity. Fig. 6 shows the results for different counter aperture diameters. The solid angle baffle A' is set in each case to give Ω = 0.59% and the variable parameter in each curve is the ring width R.

As in the previous curves, an optimum relation is indicated at the lower values of intensity; that is, for a given resolution, the maximum intensity is obtained by a proper choice of both ring width and counter aperture diameter. However, in the intensity region of primary interest, the 2.7 cm counter gives the best results. Additional measurements have shown that the counter aperture diameter may be reduced slightly below this value without appreciable effect. This indicates, in agreement with the calculations (reference 7) that the image of the source formed at the counter position is of the order of 2.7 cm diameter, and thus that the use of a larger counter would not give improved intensity.

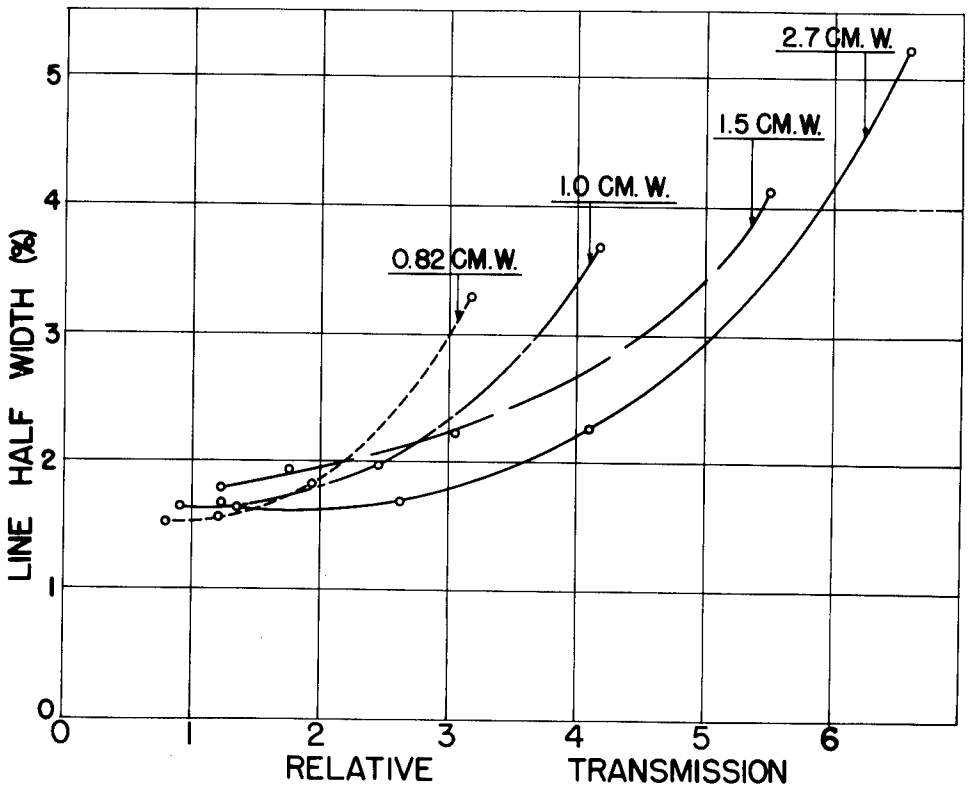

Fig. 6--Transmission-resolution relation as a function of counter diameter and ring width.

To determine the improvement effected by using ring focusing rather than axial focusing, a photoelectron source of Co^{60} was inserted into the modified spectrometer; and the peak due to the 1.3 Mev gamma-ray was determined. The baffles were adjusted to give the same half-width of 2.5% as had been obtained when this same source was measured under axial focusing conditions. After correcting for source decay, the ratio of peak intensity of the line using ring focusing to that using axial focusing was found to be 2.0. The point A on Fig. 5 represents the experimental point for axial focusing. It appears therefore that an improvement of the order of a factor of two in the intensity, at a half width of 2.5%, may be obtained by using ring focusing rather than axial focusing in a thin lens spectrometer of the type discussed here.

A question arises as to the choice of the source size to be used. It will be expected in general that in order to obtain the maximum intensity for a given line half-width, there will be an optimum source size to be used, which will depend on the half-width desired. A simple analysis, based on the assumption of vectorial addition of half-widths due to independent effects (which is valid in the case of Gaussian functions), indicates that the source size of 0.5 cm diameter is approximately optimum in the region of 2% to 3% half-width; and that the ratio of intensity to half-width is not particularly sensitive to small deviations from the optimum value.

V. INTENSITY MEASUREMENTS

A. Spectrometer Efficiency

It will be of interest to consider a quantity which may be designated as the efficiency of the spectrometer and will be denoted by the symbol e_s. The efficiency will be defined as the ratio of the counting rate observed in the spectrometercounter to the rate of emission by the source of the particles, or quanta, investigated. Three cases will be considered: The detection of internal conversion electrons, the detection of beta-rays, and the detection of gamma-rays by means of photoelectric conversion in a radiator. In the cases of internal conversion electrons and of photoelectrons due to gamma-rays, where spectral peaks are to be expected, the spectrometer efficiency will be understood to refer to

the counting rate at the peak of the spectral line. In the case of beta-rays, where no such spectral line appears, the efficiency will refer to any arbitrarily selected portion of the spectrum, and will thus be a function of the focusing current.

The following considerations will apply in each of these cases. Consider a source of monoenergetic electrons of momentum p. The probability that one of these electrons will be focused on the counter aperture will in general depend upon the momentum p, the focusing current I, the angle of emission ψ (defined as the angle between the direction of emission of the electron and the spectrometer axis), the point on the source at which the electron originated, and the angular momentum of the electron. In order to obtain an expression for the spectrometer efficiency, the following simplifying assumptions concerning the focusing action of the spectrometer will be made.

It will be assumed that the source is sufficiently small that it may be regarded as a point. It will furthermore be assumed that the baffle system is equivalent to one in which electrons in a small region of emission angles, defined by

$$\psi_1 < \psi < \psi_2$$

are selected sufficiently close to the source that the angles selected are not influenced by the magnetic field of the spectrometer; and it will be assumed that with the proper focusing current all of these electrons are focused on the counter. The work of Keller, Koenigsberg and Paskin (7) indicates that these approximations are reasonable for the purpose of a rough calculation.

If these approximations are used, and if it is recalled that for a magnetic field of a given form the trajectory of an electron with given initial conditions depends only on the ratio of momentum to field strength, then the probability that an electron with an emission angle ψ will strike the counter aperture may be written as:

$$F(\psi, p/I) = f(\psi)T(p/p_o), \qquad (1)$$

where

$$f(\psi) = 1 \quad \psi_1 < \psi < \psi_2 \qquad (2)$$

$$= 0 \text{ otherwise,}$$

and

$$T(1) = 1, \qquad (3)$$

with $$p_o = KI, \qquad (4)$$

where K is a constant known as the calibration constant of the spectrometer.

The function $T(p/p_o)$, will be called the transmission curve of the spectrometer. It is a function of p and I which designates the relative efficiency with which electrons of momentum p are focused, when the focusing current is such that the maximum counting efficiency is attained for electrons of momentum p_o. Fig. 7 shows the result of an experimental determination of the transmission curve of the spectrometer as used in the work described here. The width at half-maximum h is called the half-width of the transmission curve, and is commonly expressed in per cent.

The shape of the transmission curve may be determined experimentally as follows. A source of monoenergetic electrons of momentum p is placed in the spectrometer. The counting rate is then determined as a function of I. The counting rate to be expected at any current value I may be obtained by means of the function, $F(\psi, p/I)$:

$$N_c(I) = \int_0^{\pi} F(\psi, p/I) N_{\psi}(\psi) d\psi, \qquad (5)$$

where $N_{\psi}(\psi)d\psi$ represents the rate of emission by the source of electrons with angles between ψ and $\psi + d\psi$.[1] In the case of a very thin source of monoenergetic electrons, such as that considered here, this function is given by:

$$N_{\psi}(\psi)d\psi = 1/2\, N \sin\psi\, d\psi, \qquad (6)$$

where N is the rate of disintegration of the source. If Eqs. 1, 2 and 6 are used, Eq. 5 becomes:

$$\begin{aligned} N_c(I) &= \int_0^{\pi} f(\psi) T(p/p_o) 1/2N \sin\psi\, d\psi \\ &= 1/2\, NT(p/p_o) \int_{\psi_1}^{\psi_2} \sin\psi\, d\psi \\ &= 1/2\, NT(p/p_o)(\cos\psi_1 - \cos\psi_2), \end{aligned}$$

[1] For the purpose of simplifying the terminology, a distribution function of the form N(x)dx will, in the future, be described as "the number of (particles) in the range x,dx".

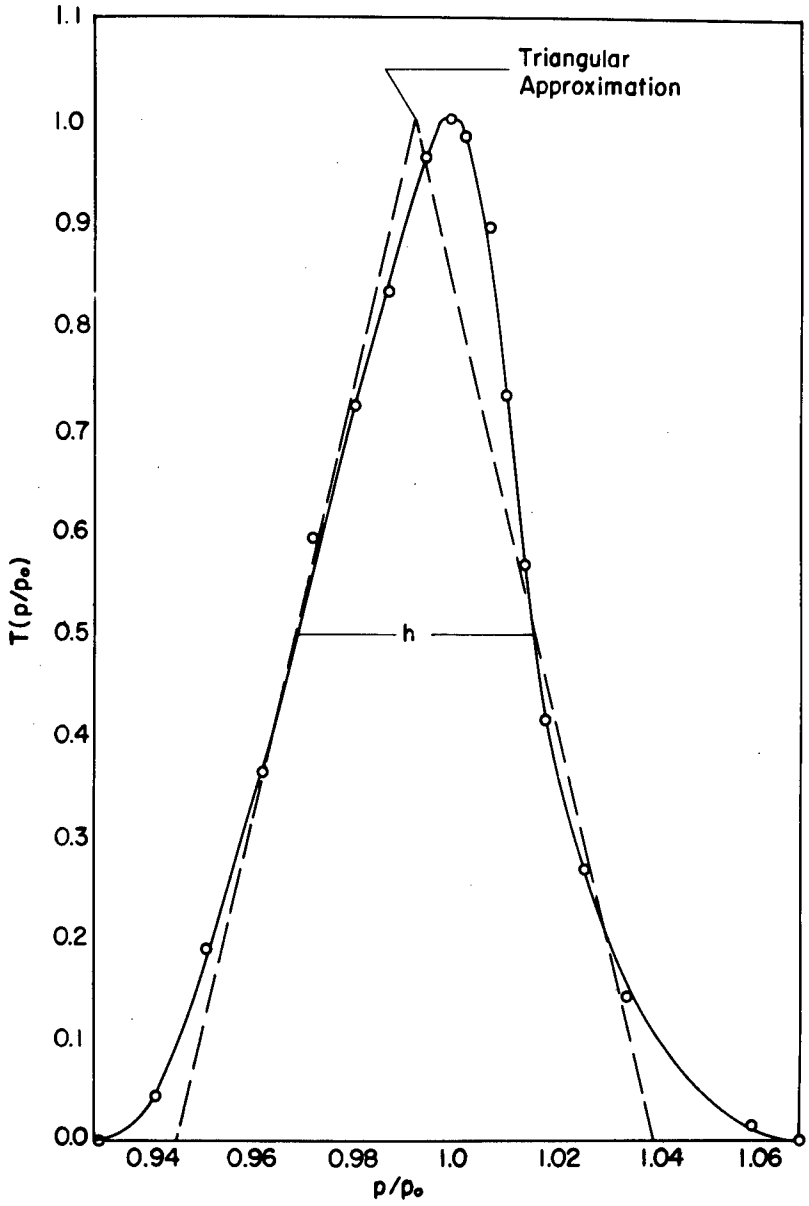

Fig. 7--Transmission curve of the beta-ray spectrometer. The triangular approximation is indicated by the dotted lines.

or $$N_c(I) = \omega NT(p/p_o), \quad (7)$$

where $$\omega \equiv 1/2(\cos \psi_1 - \cos \psi_2) \quad (8)$$

is the fractional solid angle over which electrons from the source are collected by the counter. Let the current corresponding to the maximum counting rate be given by I_o. Then from the definition of K,

$$p = KI_o. \quad (9)$$

If Eqs. 4 and 9 are substituted in Eq. 7, the result is:

$$N_c(I) = \omega NT(I_o/I). \quad (10)$$

For the special case $I = I_o$, Eq. 10 becomes:

$$N_c(I_o) = \omega NT(1) = \omega \cdot N. \quad (11)$$

If Eq. 10 is combined with Eq. 11, the result is:

$$T(I_o/I) = N_c(I)/N_c(I_o). \quad (12)$$

Thus if the ratio $N_c(I)/N_c(I_o)$ is measured as a function of I_o/I, the value of the function T is obtained. It will be observed from Eq. 12 that the observed spectral line, $N_c(I)$ resembles a reflection of the transmission curve, $T(I_o/I)$. Thus values of I less than that of the peak value I_o correspond to values of the argument of T greater than the peak value of unity.

A special case of the above described experiment results when the momentum of the electrons from the source is known. In this case, Eq. 9 may be written

$$K = p/I_o, \quad (13)$$

and thus the calibration constant K may be determined.

B. Efficiency for Detecting Internal Conversion Electrons

The spectrometer is used to measure the energy of internal conversion electrons by means of the source assembly shown in Fig. 8a. The radioactive source A is mounted, in the form of a thin film, on the source holder B. Ordinarily

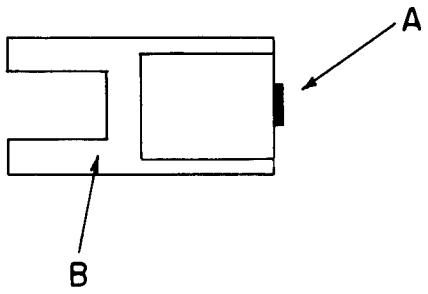

(a)

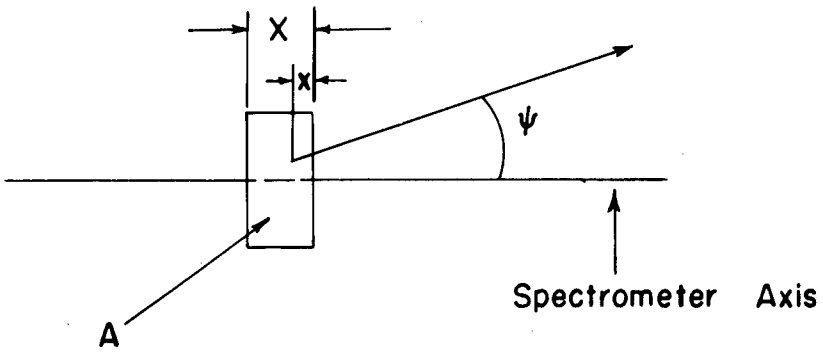

(b)

Fig. 8--Source assembly for the measurement of internal conversion electron energies.

B is a cylindrical lucite shell, on the face of which is mounted a thin plastic or aluminum foil. The source material is deposited on this foil. Monoenergetic internal conversion electrons of momentum p', originating in the source film at a depth x, will emerge at an angle ψ with respect to the spectrometer axis, as shown in Fig. 8b. If scattering of the electrons in the film is neglected, the emerging electrons will have lost a momentum Δp, given by the expression:

$$\Delta p = \frac{1}{\cos \psi} \cdot \int_o^x \frac{dp}{dx'} dx' \quad , \qquad (14)$$

where dp/dx' represents the space rate of momentum loss in the source material.

The term dp/dx' may be transformed as follows:

$$\frac{dp}{dx'} = \frac{dp}{dW} \frac{dW}{dx'} = \frac{1}{v} \frac{dW}{dx'} \quad , \qquad (15)$$

where v is the electron velocity and W is the electron energy.

Thus,

$$\frac{dp}{dx'} = \frac{\eta}{v} \quad , \qquad (16)$$

where η is the space rate of energy loss of an electron with momentum p. It should be observed that it is not necessary to carry out the transformation, Eq. 15, in order to solve the problem considered. However, since data concerning the slowing of electrons in matter are customarily given in terms of energy loss rather than momentum loss, the transformation, Eq. 15, leads to results which are more readily adaptable to numerical calculations.

Eq. 14 may now be written:

$$\Delta p = \frac{1}{\cos \psi} \int_o^x \frac{\eta}{v} dx'. \qquad (17)$$

The momentum of the emerging electrons is then:

$$p = p' - \Delta p = p' - \frac{1}{\cos \psi} \int_o^x \frac{\eta}{v} dx'. \qquad (18)$$

The use of Eq. 18 implies a unique relationship between the momentum of the electron and its position in the source film. Such a relationship does not actually exist, since the loss of energy of an electron in passing through matter is a statistical process, and may vary between wide limits in different cases under the same conditions. Thus to make use of the expression developed here, it will be necessary to use a suitable average value for the energy loss of an electron as a function of the electron energy and of the material through which it passes.* From Eq. 18, the momentum distribution of the electrons emerging from the face of the source film may be obtained. Electrons originating at a depth in the range x, dx, with a momentum p', will emerge with momenta in the range p, dp, where from Eq. 18,

$$dp = \frac{1}{\cos\psi} \quad \frac{\eta}{v} \quad dx. \qquad (19)$$

Now consider the electrons originating at a depth in the range x, dx with emission angles in the range ψ, $d\psi$. These electrons will emerge with the distribution

$$N_x dx \cdot 1/2 \sin\psi \quad d\psi ,$$

where N_x is the source rate of emission of electrons per unit source thickness. If Eq. 19 is used, the distribution in momentum and emission angle of the emerging electrons becomes:

$$N_{p,\psi} \quad (p, \psi)dpd\psi \quad = N_x \cos\psi \quad \cdot \frac{v}{\eta}dp \cdot 1/2 \sin\psi \, d\psi, \qquad (20)$$

---

*It has been customary in this laboratory to use the average energy loss as given by Heitler (24). Hornyak, Lauritsen and Rasmussen (25) have suggested that, since the average loss is appreciably affected by a relatively small number of electrons suffering extremely large losses, the most probable loss would be a more reasonable value to employ. Work in this laboratory (reference 26), however, has indicated that the use of the most probable loss does not give as good agreement with experiment as the use of the average loss. It is possible that the effect of scattering, which tends to lengthen the electron path in a foil, may be compensated for to some extent by the use of the average loss rather than of the most probable loss.

where $N_{p,\psi}(p, \psi)dp\, d\psi$ is the rate of emergence of electrons with momenta in the range p, dp and emission angles in the range ψ, $d\psi$. The rate at which these electrons arrive at the counter is given by

$$F(\psi, p/I)\, N_{p,\psi}(p, \psi)dp\, d\psi .$$

If the efficiency with which these electrons are counted by the counter is designated by $e_c(p)$, the counting rate is given by:

$$N_{IC}(I) = \int_0^{\pi} d\psi \int_{p_1}^{p_2} dp\, F(\psi, p/I)\, N_{p,\psi}(p, \psi) e_c(p). \tag{21}$$

The integral over p is to be taken over all momenta represented in the distribution. The upper limit p_2 is represented by electrons emerging from zero depth, x = 0. Thus:

$$p_2 = p'. \tag{22}$$

The lower limit p_1 is represented by electrons emerging from the depth x = X, where X is the thickness of the source film. From Eq. 18, p_1 is given by:

$$p_1 = p' - \frac{1}{\cos\psi} \int_0^X \frac{\eta}{v}\, dx' = p' - \delta, \tag{23}$$

where

$$\delta \equiv \frac{1}{\cos\psi} \int_0^X \frac{\eta}{v}\, dx'. \tag{24}$$

If Eqs. 1, 20, 22 and 23 are used, Eq. 21 becomes:

$$N_{IC}(I) = 1/2\, N_x \int_0^{\pi} d\psi\, f(\psi) \sin\psi \cos\psi \int_{p'-\delta}^{p'} dp T(p/p_o) \frac{v}{\eta} e_c(p).$$

Due to Eq. 2, this may be written:

$$N_{IC}(I) = 1/2\, N_x \int_{\psi'}^{\psi_2} d\psi \sin\psi \cos\psi \int_{p'-\delta}^{p'} dp T(p/p_o) \frac{v}{\eta} e_c(p). \tag{25}$$

Since ψ_1 and ψ_2 are ordinarily both of the order of 0.1 radian, there will be an error of the order of only 1% if $\cos \psi$ is taken as unity. Then from Eq. 24,

$$\delta \cong \int_0^X \frac{\eta}{v} \, dx'. \qquad (26)$$

If this approximation is made in Eq. 25, then the integral over p is independent of ψ and the integrals may be iterated. The result is:

$$N_{IC}(I) = N_X(G(I)) \cdot \omega \quad , \qquad (27)$$

where

$$\omega = 1/2 \int_{\psi_1}^{\psi_2} \sin \psi \, d\psi = 1/2 \, (\cos \psi_1 - \cos \psi_2), \qquad (28)$$

and

$$G(I) = \int_{p'-\delta}^{p'} T(p/p_o) \, \frac{v}{\eta} \, e_c(p) \, dp. \qquad (29)$$

Contributions to the integral will occur only for values of p where the integrals all differ from zero. The design of the spectrometer is such that $T(p/p_o)$ differs from zero only in the region where $|1 - p/p_o| \lesssim .05$. This corresponds to variations of p of the order of a few per cent. Since v, η and e_c do not in general change rapidly over this range of momenta, the term

$$\frac{v \, e_c(p)}{\eta}$$

may be considered constant:

$$\frac{v \, e_c(p)}{\eta} \cong \frac{v(p') \, e_c(p')}{\eta \, (p')} \quad ,$$

if it is understood that the integral G is being evaluated in the region $p_o \cong p'$. The result of this approximation is indicated by the dotted rectangle in Fig. 9. It has been found experimentally (Fig. 7) that the transmission curve $T(p/p_o)$ may be closely approximated by an isoceles

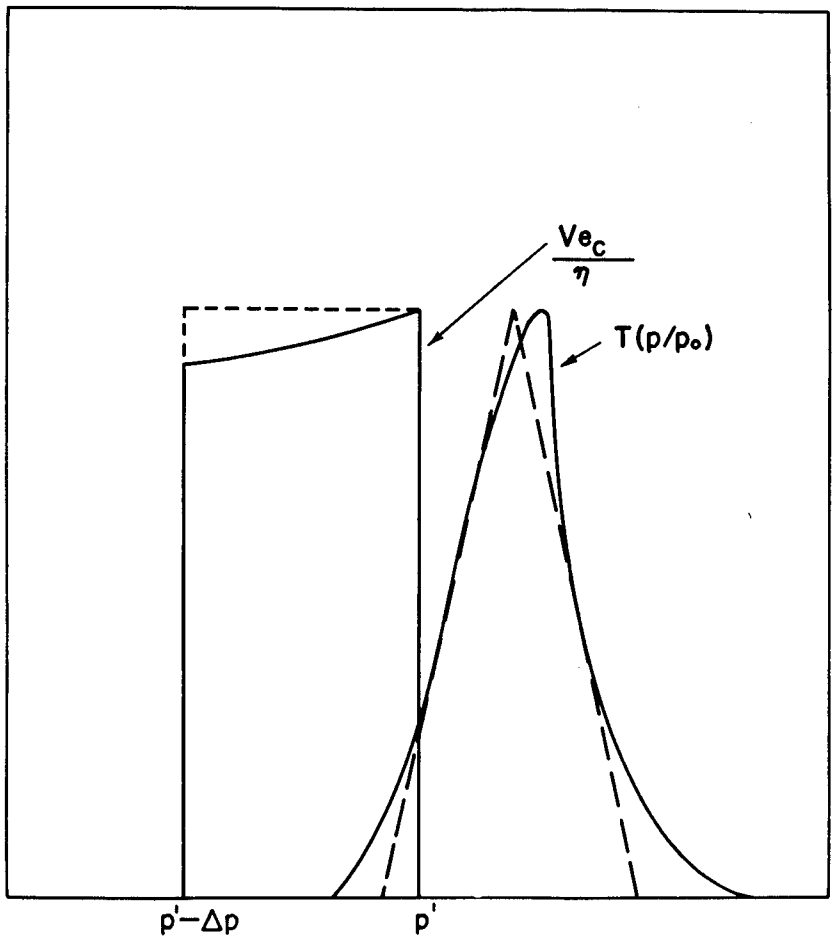

Fig. 9--Momentum distribution and transmission curve for the case of internal conversion electrons. The dotted lines indicate approximations used in the evaluation of the spectrometer efficiency.

triangle, with half-width $\Delta(\frac{p}{p_o}) = h$, where h is the experimentally determined half-width of the actual transmission curve. The result of this approximation is indicated by the dotted triangles in Figs. 7 and 9. If these approximations are made, Eqs. 29 and 26 become:

$$G(I) = \frac{v(p')\, e_c(p')}{\eta(p')} \int_{p'-\delta}^{p'} T(p/p_o)\,dp, \qquad (30)$$

and

$$\delta = \frac{\eta(p')X}{v(p')}, \qquad (31)$$

Jensen (3) has shown that, in this case, the value of I corresponding to the maximum of G is given by:

$$I_o \cong \frac{1}{K}(p' - \delta/2) \text{ or } p_o = p' - \delta/2, \quad 2hp' > \delta,$$

$$I_o \cong \frac{1}{K}(p' - hp_o) \text{ or } p_o = p'/(1 + h), \quad 2hp' < \delta.$$

The corresponding value, $G(I_o)$, of G is easily found by integrating the triangle $T(p/p_o)$ between $p' - \delta$ and p'. The result is:

$$G(I_o) = \frac{h\, p'\, v\, e_c}{\eta} \qquad \alpha > 1$$

$$= (1 - \frac{\alpha}{2})e_c X \qquad \alpha < 1, \qquad (32)$$

where

$$\alpha \equiv \frac{\eta\ X}{2\,h\,v\,p'} = \frac{\delta}{2\,h\,p'} \qquad (33)$$

is the ratio of the momentum loss in the source, δ, to the base of the transmission curve, 2 h p'.

The counting rate at the peak of the spectral line may now be written:

$$N_{IC}(I_o) = N_x \omega G(I_o)$$

$$= \frac{N_x \omega h p' v e_c}{\eta}, \quad \alpha > 1$$

$$= N_x \omega e_c(1 - \frac{\alpha}{2}), \quad \alpha < 1. \qquad (34)$$

Since the total source strength N is given by

$$N = N_x X,$$

the efficiency,

$$e_s(IC) = \frac{N_{IC}(I_o)}{N},$$

becomes

$$e_s(IC) = \frac{\omega h p' v e_c}{\eta X}, \quad \alpha > 1$$

$$= \omega e_c(1 - \frac{\alpha}{2}), \quad \alpha < 1, \qquad (35)$$

where

$$\alpha = \frac{\eta X}{2 h v p'}.$$

C. Efficiency for Detecting Beta-Rays

The continuous distribution of electrons, characteristic of beta-decay, is analysed with the same source assembly described in the case of internal conversion electrons. The parent distribution of electrons, however, instead of consisting of a group of monoenergetic electrons of momentum p', is characterised by a distribution function

$$n(p')dp',$$

where n(p') is the rate at which electrons in a unit momentum interval, centered about the momentum p', are emitted by the source. The counting rate, at a given focusing current I, is obtained by integrating Eq. 27 over all momenta, p'. The source strength N_x must in this case be multiplied by the factor

$$\frac{n(p')dp'}{N}$$

(which represents the fraction of the emitted electrons in the momentum range p', dp'), where N is the total rate of emission of beta-particles. The resulting counting rate is then:

$$N_\beta(I) = \frac{\omega N_x}{N} \int_o^\infty G(I)n(p')dp' = \frac{\omega}{X} \int_o^\infty G(I)n(p')dp'. \tag{36}$$

From Eq. 29, this becomes:

$$N_\beta(I) = \frac{\omega}{X} \int_o^\infty n(p') \int_{p'-\delta}^{p'} T(p/p_o) \frac{v}{\eta} e_c \, dp \, dp'. \tag{37}$$

Since $T(p/p_o)$ differs from zero only for $p \cong p_o$, this may be written approximately:

$$n_\beta(I) = \frac{\omega}{X} \frac{v(p_o)}{\eta(p_o)} e_c(p_o) \int_o^\infty n(p') \int_{p'-\delta}^{p'} T(p/p_o)dp \, dp'. \tag{38}$$

Consider now the case in which

$$\delta(p' \cong p_o) \ll hp_o. \tag{38a}$$

This case is illustrated in Fig. 10. The integral over p is approximately $\delta \cdot T(p'/p_o)$.

The integral over p' is then

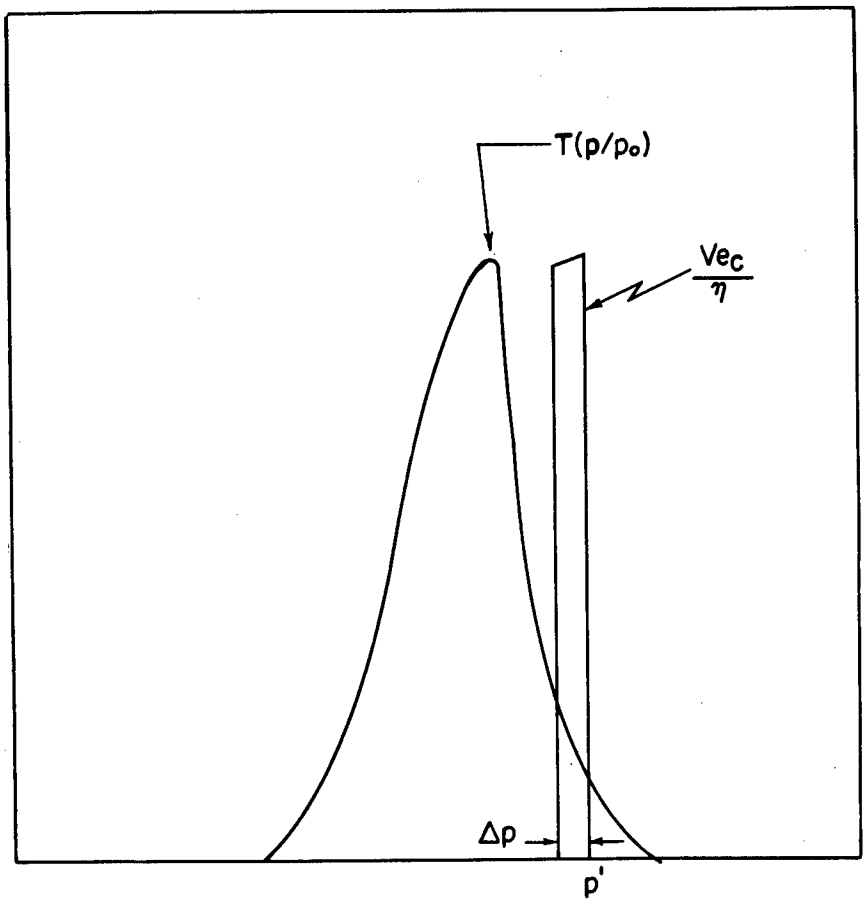

Fig. 10--Momentum distribution and transmission curve for the case of beta rays.

$$\int_0^\infty n(p')\ \delta\ T(p'/p_o)\ dp'.$$

Since $n(p')$ and δ are ordinarily slowly varying functions of p' compared to $T(p'/p_o)$ (as long as the upper energy limit of the beta-spectrum is avoided), these terms may be removed from the integral. The result is

$$\delta\ n(p_o) \int_0^\infty T(p'/p_o)\ dp',$$

or

$$\delta\ n(p_o)\ p_o \int_0^\infty T(x)\ dx.$$

where δ is to be evaluated for $p' \cong p_o$.

If this expression is inserted in Eq. 38, there results:

$$N_\beta(I) = \frac{\omega}{X}\ \frac{v(p_o)}{\eta(p_o)}\ e_c\ (p_o)\ \delta(p' \cong p_o)\ n(p_o)p_o \int_0^\infty T(x)dx. \qquad (39)$$

The term δ is given by Eq. 31:

$$\delta(p' \cong p_o) = \frac{\eta(p_o)X}{v(p_o)}\ .$$

The term $\int_0^\infty T(x)dx$

is simply the area under the transmission curve. This may be obtained by numerical integration of the experimentally transmission curve, or, if the triangular approximation is

used, it may be taken as the half-width h. Eq. 39 becomes:

$$N_\beta(I) = \omega\, e_c(p_o)\, n(p_o)\, p_o h. \qquad (40)$$

Since $p_o = KI$, this may be written:

$$\frac{N_\beta(I)}{I} = \omega\, e_c(p_o)\, n(p_o)\, Kh. \qquad (41)$$

Thus, if the counter efficiency e_c is independent of energy, Eq. 41 shows that the ratio

$$N_\beta(I)/I$$

is proportional to the momentum distribution function, $n(p_o)$.

Consider now the case in which the inequality $\delta(p' \cong p_o) \ll p_o$ is satisfied, but the inequality $\delta(p' \cong p_o) \ll hp_o$ is not satisfied. This is the case in which the momentum loss in the source is much less then the focused momentum p_o, but is not much less than the width of the transmission curve. Under these conditions it is to be expected that electrons which originate with a momentum p' in the deeper layers of the source and emerge with a momentum $p' - \Delta p$ will be partially compensated for by electrons which originate with a momentum $p' + \Delta p$ and emerge with a momentum p'.* Thus for sources of moderate thickness ($\delta \ll p_o$) the observed counting rate will be expected to be approximately the same as for thin sources ($\delta \ll hp_o$) of the same total activity; and Eqs. 40 and 41 will still apply in these cases. As in the case of the thin source previously considered, these considerations will not apply in the immediate neighborhood of the upper energy limit of the beta-spectrum.

---

*Due to the slope of the parent beta-ray distribution, particles originating with a momentum $p' + \delta$ will differ in abundance from those originating with a momentum p' by a term $(\delta/p')dn(p)/d(\ln p)$. Thus a term of this order of magnitude is neglected in the above discussion.

The counting rate in the spectrometer, when it is focused on a region of a beta-spectrum, is thus given by Eq. 40:

$$N_\beta(I) = \omega\, e_c(p_o)\, n(p_o)\, p_o h, \tag{40}$$

with the condition $\delta\,(p' \cong p_o) \ll p_o$.

If the efficiency of the spectrometer is designated by:

$$e_s(\beta) \equiv \frac{N_\beta(I)}{N},$$

then from Eq. 40, and since

$$N = \int_o^\infty n(p_o)\, dp_o,$$

the following result is obtained:

$$e_s(\beta) = \omega\, e_c(p_o)\, \frac{h p_o\, n(p_o)}{\int_o^\infty n(p_o)\, dp_o}. \tag{42}$$

If a thin source only is considered ($\alpha \ll 1$), it is seen by comparison with Eq. 35 that the spectrometer efficiency is reduced from that for counting internal conversion electrons by a factor:

$$\frac{h p_o\, n(p_o)}{\int_o^\infty n(p_o)\, dp_o}. \tag{42a}$$

This is, of course, due to the fact that only a fraction of the order of h of the beta-particles are counted at any current setting. The reduction factor (42a) may be computed from the measured half-width, h, of the transmission curve and from the measured shape of the beta-ray momentum distribution.

D. Efficiency for Detecting Gamma-Rays

A common method of gamma-ray analysis with the spectrometer involves the use of a source assembly such as that shown in Fig. 11. The source material A is deposited in a container B of low atomic number. On the face of B is attached a radiator foil C of high atomic number. The container B is made sufficiently thick to stop any electrons emitted by the source. Gamma-rays undergo the processes of Compton scattering and photoelectric absorption in B and in C. The container B is constructed of a light element to minimize the effect of photoelectric absorption, and the radiator C is ordinarily a heavy element to favor the photoelectric effect. The photoelectrons produced in C will have an energy

$$E = E_\gamma - B.E.,$$

where E_γ is the photon energy and B.E. is the binding energy of the emitted photoelectrons. By measuring the energy E, it is possible to deduce the gamma-ray energy E_γ.

It is of interest to determine the number of photoelectrons counted by the spectrometer counter due to a source emitting N quanta of energy E_γ per unit time. Consider a quantum emitted at an angle between θ and θ and $d\theta$ with respect to the spectrometer axis. The number of such quanta is given by:

$$P_1(\theta)\, d\theta = 1/2\ N \sin\theta\, d\theta. \qquad (43)$$

The probability that this quantum will emit a photoelectron from the K shell of an atom of the radiator, at a depth x in the radiator, is given by:

$$P_2(x,\theta)\, dx = \frac{1}{\cos\theta}\, \tau_K\, dx\ , \qquad (44)$$

where τ_K is the absorption coefficient of the raidator for photoelectron emission from the K shell. Let the probability that this electron be emitted at an angle between ϕ and $\phi + d\phi$ with respect to the direction of the photon be designated by

$$P_3(\phi)\, d\phi. \qquad (44a)$$

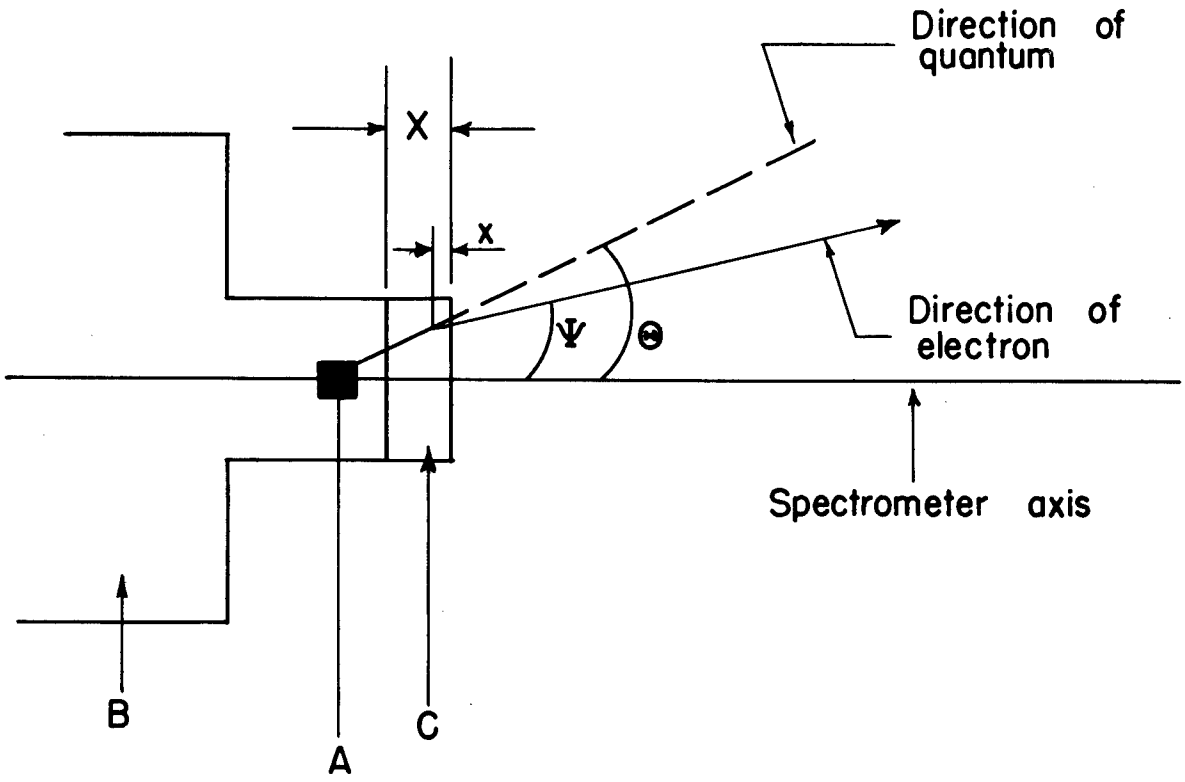

Fig. 11--Source assembly for the measurement of gamma-ray energies.

If scattering is neglected, the electron will emerge from the face of the radiator with its direction unchanged. A certain fraction of such electrons will emerge at an angle ψ with respect to the spectrometer axis, such that

$$\psi_1 < \psi < \psi_2 . \tag{44b}$$

Let this fraction be designated by

$$P_4(\theta, \phi, \psi_1, \psi_2). \tag{44c}$$

The fraction of the electrons satisfying the condition (44b), which reach the counter is given by the transmission curve of the spectrometer:

$$P_5(p) = T(p/p_o). \tag{44d}$$

The fraction of these which is counted is given by the counter efficiency:

$$P_6(p) = e_c(p). \tag{45}$$

The spectrometer counting rate is then given by forming the product

$$P_1 P_2 \cdots P_6,$$

and integrating over all of the variables. The result is

$$N_r = \int_o^{\pi} d\theta \; 1/2 \; N \sin\theta \int_o^{X} dx \, \frac{\tau_K}{\cos\theta} \int_o^{\pi} d\phi P_3(\phi) P_4(\theta, \phi \; \psi_1, \psi_2) \; T\left(\frac{p}{p_o}\right) e_c(p). \tag{46}$$

Before attempting to evaluate the integral it is necessary to express the variable p in terms of the other variables. This is done in the same way as in the case of internal conversion electrons discussed above. The result is:

$$N_\gamma = \int_0^{\theta_o} d\theta \; 1/2 \; N \sin\theta \int_{p'-\delta}^{p'} \frac{v}{\eta} \frac{\tau_K}{\cos\theta} dp \int_0^{\pi} d\phi P_3(\phi) P_4(\theta,\phi,$$

$$\psi_1, \psi_2) T(p/p_o) e_c(p) = N \tau_K \omega_e \int_{p'-\delta}^{p'} \frac{v}{\eta} T(p/p_o) e_c(p) \, dp, \tag{47}$$

where

$$\omega_e = 1/2 \int_0^{\theta_o} \tan\theta \int_0^{\pi} P_3(\phi) P_4(\theta,\phi, \psi_1, \psi_2) \, d\phi \, d\theta, \tag{48}$$

and θ_o is the angle subtended by the radiator at the source. The integral over p has been evaluated in section V .B, and, if the maximum counting rate only is considered, is given by Eq. 32:

$$G(I_o) = \frac{h \, p' \, v \, e_c}{\eta}, \qquad \alpha > 1$$

$$= e_c \, X(1 - \alpha/2), \qquad \alpha < 1. \tag{49}$$

Eq. 47 becomes:

$$N_\gamma(I_o) = N \tau_K \omega_e G(I_o), \tag{50}$$

or

$$N_\gamma(I_o) = \frac{N \tau_K \omega_e \, h \, p' \, v \, e_c}{\eta}, \qquad \alpha > 1 \tag{51}$$

$$= N \tau_K \omega_e \, e_c \, X(1-\alpha/2), \qquad \alpha < 1,$$

where as before:

$$\alpha \equiv \frac{\eta X}{2 \, h \, v \, p'}. \tag{52}$$

The evaluation of the integral ω_e will be considered for two limiting cases.

Consider first the non-relativistic case,

$$v/c << 1,$$

where v is the velocity of the photoelectron considered and c is the velocity of light. It is in this region that electron scattering will be of primary importance. Scattering will tend to destroy the angular dependence of the electrons on the angles θ and ϕ.* Thus let it be assumed that the electrons emerging from the radiator have an isotropic distribution in angle. The integral

$$\int_0^{\pi} P_3(\phi) P_4(\theta, \phi, \psi_1, \psi_2)\, d\phi$$

is the probability that an electron emerge from the radiator with an emission angle ψ such that

$$\psi_1 < \psi < \psi_2 .$$

Since it is assumed that the angular distribution of the emerging electrons is isotropic, this term is simply the fractional solid angle subtended by ψ_1 and ψ_2. Thus

$$\int_0^{\pi} P_3(\phi) P_4(\theta, \phi, \psi_1, \psi_2)\, d\phi = \omega .$$

The term ω_e then becomes:

$$\omega_e = \frac{\omega}{2} \int_0^{\theta_o} \tan \theta \, d\theta = \frac{\omega}{2} \ln \sec \theta_o . \qquad (53)$$

*It must also be noted that scattering will, in this case, have a considerable effect in increasing the electron path length, and will thus give rise to excessive energy losses in the radiator. This will undoubtedly destroy the rectangular momentum distribution which is being assumed. The results in this case will have a qualitative significance only.

The term ln sec θ_o may be determined from the geometry of the source assembly and is typically of the order of 0.75 to 1.5. Thus:

$$\omega_e = a\,\omega,$$

where $a = 1/2$ ln sec θ_o is of the order of 0.4 to 0.8. Since this case is one in which scattering is important, and since the effect of scattering has not been taken into account in the consideration of energy loss in the radiator, the approximation probably does not justify considering the effect of the factor a. For this case, therefore, a will be taken as unity:

$$\omega_e \cong \omega. \tag{54}$$

Consider next the relativistic case,

$$\frac{v}{c} \cong 1.$$

For this case there is a preponderance of photoelectric emission in the forward direction. The function $P_3(\phi)$ approaches the Dirac delta function:

$$P_3(\phi) \cong \delta(\phi,0), \tag{55}$$

where $\delta(\phi,\phi')$ is defined such that

$$\int_{a<\phi'}^{b>\phi'} F(\phi)\,\delta(\phi,\phi')\,d\phi = F(\phi'),$$

where F is an arbitrary function. If Eq. 55 is inserted in Eq. 48, the result is:

$$\omega_e = 1/2 \int_o^{\theta_o} \tan\theta\, P_4(\theta,0,\psi_1,\psi_2)\, d\theta. \tag{56}$$

But from the definition of P_4,

$$P_4(\theta, 0, \psi_1, \psi_2) = 1, \qquad \psi_1 < \theta < \psi_2$$

$$= 0, \text{ otherwise.}$$

Eq. 56 thus becomes:

$$\omega_e = 1/2 \int_{\psi_1}^{\psi_2} \tan \theta \, d\theta,$$

and since ψ_1 and ψ_2 are both of the order of 0.1,

$$\tan \theta \cong \sin \theta;$$

and thus:

$$\omega_e \cong 1/2 \int_{\psi_1}^{\psi_2} \sin \theta \, d\theta = 1/2 \, (\cos \psi_1 - \cos \psi_2) = \omega. \tag{57}$$

If Eqs. 54 and 57 are taken into account, Eq. 51 becomes:

$$N_\gamma(I_o) = \frac{N \tau_K \, h \, p' \, v \, e_c \, \omega}{\eta}, \qquad \alpha > 1$$
$$= N \, \tau_K \, e_c \, X(1 - \alpha/2), \qquad \alpha < 1, \tag{58}$$

with

$$\alpha \equiv \frac{\eta X}{2 \, h \, v \, p'};$$

and the spectrometer efficiency for the detection of the gamma-radiation due to photoelectric conversion in the K shell becomes:

$$e_s(\gamma) = \frac{\tau_K \, h \, p' \, v \, e_c \, \omega}{\eta}, \qquad \alpha > 1$$
$$= \tau_K \, e_c \, \omega \, X(1 - \alpha/2), \qquad \alpha < 1. \tag{59}$$

A similar expression is obtained for the case of photoelectric conversion in the L shell, M shell, etc.

E. Summary

The Eqs. 35, 42 and 59 may be rewritten in the following forms:

$$e_s(IC) = [\omega e_c] \; S(\alpha) \; , \tag{60}$$

$$e_s(\beta) = [\omega e_c] [h \; p_o \; n(p_o)/N] \; , \tag{61}$$

$$e_s(\gamma) = [\omega e_c] \; S(\alpha) \; [\tau \cdot X] . \tag{62}$$

The notation used is as follows:

The term,

$$\omega = 1/2 \; (\cos \psi_1 - \cos \psi_2)$$

is the fractional solid angle characteristic of the angle of acceptance of the spectrometer for electrons of momentum

$$p_o = KI .$$

This solid angle is of the order of 1%.

The term e_c is the intrinsic efficiency of the counter for counting electrons of momentum p_o. In the case of a Geiger counter, of not too low a pressure, it is characterized by a value close to unity for electron energies above a critical energy. Below this energy, which is typically of the order of 25 to 50 Kev, the transmission of the counter window decreases sharply with decreasing energy, with a corresponding decrease in e_c.

In Eq. 61, which refers to the detection of beta-rays, $n(p_o)$ is the rate of emission of electrons in a unit momentum interval centered about the momentum p_o.

N is the total source strength, given by:

$$N = \int_o^\infty n(p_o) \; dp_o .$$

In Eq. 62, τ is the absorption coefficient for the photoelectric effect from the orbital shell under consideration, and X is the thickness of the radiator.

The term α is defined by:

$$\alpha = \frac{\eta X}{2 h \nu p'} \cong \frac{\eta X}{2 h \nu p_o} , \qquad (63)$$

where X is the thickness of the source in the case of internal conversion electrons, and of the radiator in the case of photoelectrons.

The function $S(\alpha)$ is obtained from Eq. 35 or Eq. 59, and is given by:

$$\begin{aligned} S(\alpha) &= (1 - \alpha/2), && \alpha < 1 \\ &= 1/2\alpha , && \alpha > 1 . \end{aligned} \qquad (64)$$

In each case the efficiency is seen to contain the factor ωe_c. This factor is the probability with which electrons from a monoenergetic source are counted if the focusing current is of such a value as to focus them most efficiently.

In the case of internal conversion electrons, the factor ωe_c is multiplied by the function $S(\alpha)$, which depends upon the electron momentum, the source thickness, and the source material. This function gives the effect of energy loss in the source. It is seen to reduce to unity for very thin sources.

In the case of beta-rays, the factor $S(\alpha)$ is not involved in the order of approximation used here. The factor ωe_c is multiplied by a factor involving the form of the beta-spectrum. This factor gives the fraction of the beta-spectrum which lies within the transmission curve of the spectrometer.

In the case of photoelectrons due to gamma-rays, the same factors are involved as in the case of internal conversion electrons, with the exeption that the terms in $S(\alpha)$ refer to the radiator material and thickness rather than those of the source. In addition there is a factor τX, which is seen to be the probability with which a photo-

electron is produced by a photon in passing through the radiator.

Due to the fact that the effect of electron scattering in the source material (or in the radiator) has been neglected throughout, it is not suggested that the above expressions for the spectrometer efficiency will be useful for accurate calculations. They do, however, furnish an order of magnitude estimate of counting rates to be expected under given conditions. In addition they serve to indicate many of the qualitative features of intensity relations, such as the decrease of efficiency for internal conversion electrons with increasing source thickness. Lastly, these relations furnish interpolation formulae for the interpretation of experimental data. Thus if effective values of α in Eqs. 60 and 62 are determined experimentally for various combinations of energy, source material and source thickness, it may be anticipated that these formulae will apply with some degree of rigor.

VI. COINCIDENCE COUNTING

A. Introduction

The method of coincidence counting in the analysis of nuclear decay schemes has been discussed by many authors (9-18). The basic experimental arrangement is customarily as indicated in Fig. 12. A radioactive source is placed at some position such that its radiations may impinge upon the counters C_1 and C_2. Particles which are detected by these counters give rise to electrical pulses which are recorded by the registers R_1 and R_2. These pulses are also transmitted to the coincidence circuit R_c. This circuit is of such a nature that a pulse arriving from C_1 at a time t and a pulse arriving from C_2 at a time $t \pm \Delta t$ will cause the coincidence circuit to register if and only if $\Delta t < \tau_c$, where τ_c is a characteristic of the coincidence circuit known as the resolving time. By means of this basic arrangement it is possible to determine whether two particles are emitted within a time τ_c, implying a cascade transition, or whether there is no observable time correlation, implying a parallel transition or a metastable state. Since the resolving time τ_c is customarily of the order of 10^{-6} sec., and since the half-life for allowed gamma-emission is of the order

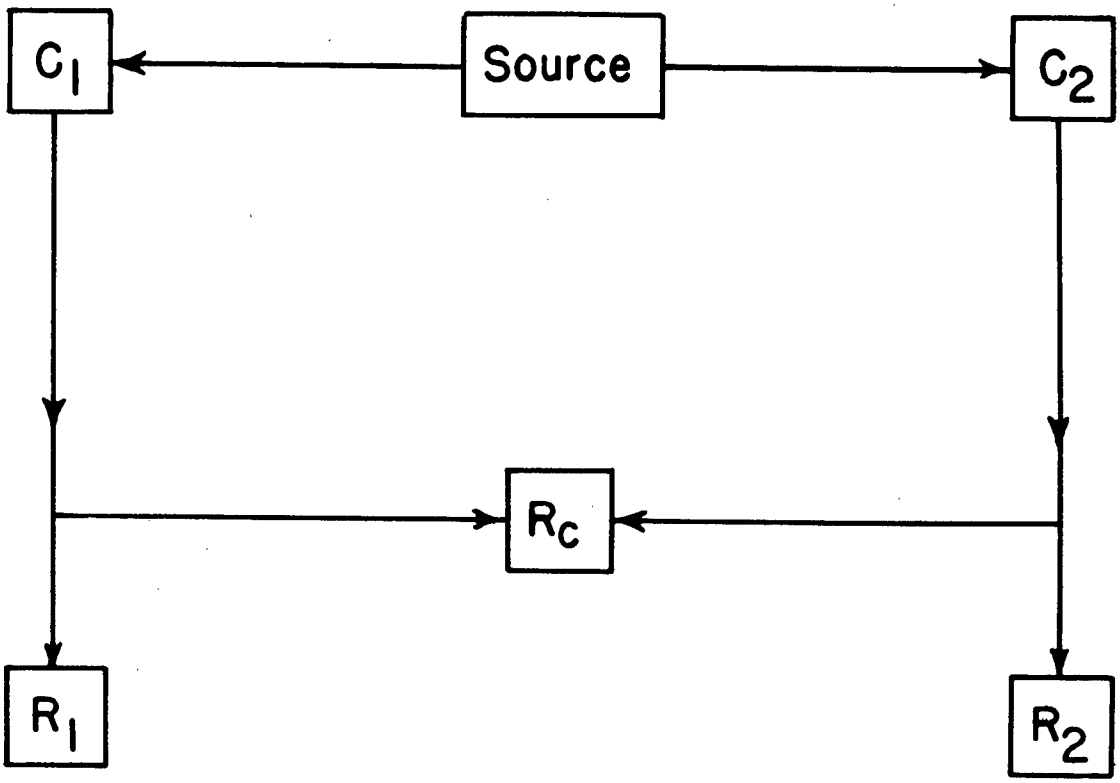

Fig. 12--Block diagram of coincidence counting system.

of 10^{-13} sec., the time between a beta- or a gamma-transition and a succeeding allowed gamma-transition is always much less than τ_c. When this is the case the particles are said to be "in coincidence" with each other.

It must be observed that even though there may be no particles in coincidence with each other, there will still be a finite counting rate in the coincidence circuit, due to the random probability of an actuation of C_1 and an actuation of C_2 within the time τ_c. It can be easily shown (Korff (28, p. 145)) that this "accidental" coincidence rate is given by:

$$N_a = 2 \tau_c N_1 N_2, \tag{65}$$

where N_1 and N_2 are the counting rates in C_1 and C_2 respectively.

Consider a source which decays at the rate of N disintegrations per unit time. Let each separate transition be designated as a "particle of type i", where i varies between 1 and n, and n is the number of different transitions. Let n_i be the number of transitions of type i per unit time. Let a_{ij} be the probability per transition that a particle of type i is in coincidence with a particle of type j. The quantities n_i and a_{ij} are then purely characteristic of the radioactive isotope involved, while N is both a characteristic of the radioactive isotope and of the quantity of material present. Let N_1 be the counting rate in C_1, and let N_2 be the counting rate in C_2. Let N_c be the counting rate in the coincidence circuit due to particles which are actually in coincidence with each other; let N_a be the accidental coincidence rate; and let N_o be the observed coincidence rate. Let e_{1i} be the efficiency of C_1 for particles of type i (where the efficiency of the counter is taken to include the solid angle factor), and let e_{2i} be similarly defined for C_2.

Then:

$$N_o = N_c + N_a, \tag{66}$$

$$N_1 = N \sum_i n_i e_{1i}, \tag{67}$$

$$N_2 = N \sum_j n_j e_{2j}, \tag{68}$$

$$N_c = N \sum_i \sum_j a_{ij}\, e_{1i}\, e_{2j}. \qquad (69)$$

Also, from Eq. 65:

$$N_a = 2 \tau_c N_1 N_2$$

$$= 2 \tau_c N^2 \sum_i n_i\, e_{1i} \sum_j n_j\, e_{2j}. \qquad (70)$$

The problem of determining the decay scheme of a particular isotope consists in determining the coefficients n_i and a_{ij}. The coefficients n_i may, in principle, be determined by means of energy measurements in the beta-ray spectrometer, and through the use of intensity relations such as those discussed in section V. To determine the coefficients a_{ij} it is necessary to resort to coincidence measurements. This may be done, in principle, by counting coincidences and varying the efficiencies e_{1i} and e_{2j} in Eqs. 67-69.

It will be of interest to consider a particular example of the application of Eqs. 66-70. Consider the known decay scheme (Deutsch, Elliott and Roberts (29)) of Co^{60} as indicated in Fig. 13. A beta-ray transition is followed by two gamma-ray transitions. All of these processes occur in cascade in a time believed to be of the order of 10^{-13} sec., so that all three particles may be said to be in coincidence. From Fig. 13, if gamma-ray No. 1, is particle 1, gamma-ray No. 2 is particle 2, and the beta-ray is particle 3, then the decay coefficients n_i and a_{ij} become:

$$n_1 = n_2 = n_3 = 1,$$

$$a_{12} = a_{13} = a_{23} = 1.$$

Suppose that C_1 is a gamma-counter which will count gamma-1 and gamma-2 with an efficience e_γ. Since the energies of gamma-1 and gamma-2 are nearly equal, and since the efficiency of a Geiger counter varies more or less linearly with energy (Von Droste (30)), e_{11} and e_{12} will be approximately equal. Let C_2 be a beta-counter which will count the beta-rays from Co^{60} with an efficiency e_β, and will count gamma-rays with an efficiency ae_β, where $a \ll 1$. Then:

$$e_{11} = e_{12} = e_\gamma, \quad e_{13} = 0, \qquad (71)$$

$$e_{21} = e_{22} = ae_\beta, \quad e_{23} = e_\beta. \qquad (72)$$

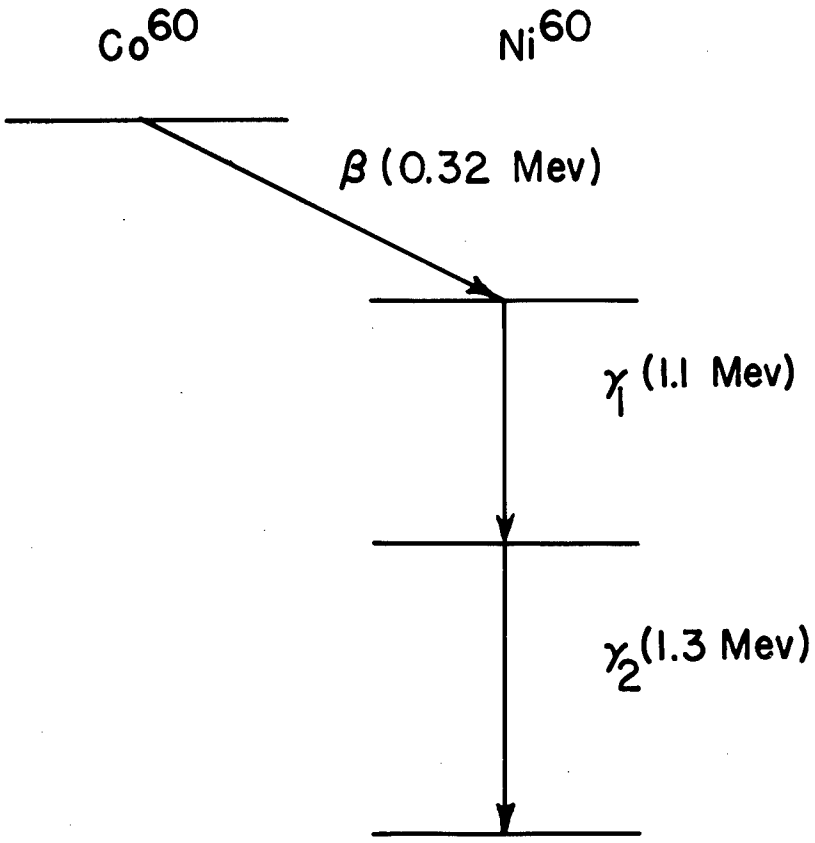

Fig. 13--Decay scheme of Co^{60}.

Eqs. 67-69 then become:

$$N_1 = 2 N e_\gamma , \tag{73}$$

$$N_2 = N(2ae_\beta + e_\beta) \cong N e_\beta , \tag{74}$$

$$N_c = N(2 e_\beta e_\gamma + 4 ae_\beta e_\gamma) \cong 2 N e_\beta e_\gamma . \tag{75}$$

From Eqs. 73-75 it is possible to determine the three quantities N, e_γ and e_β from measured values of N_1, N_2 and N_c. Thus:

$$N = N_1 N_2/N_c, \tag{76}$$

$$e_\beta = N_c/N_1, \tag{77}$$

$$e_\gamma = N_c/2N_2. \tag{78}$$

It is of course necessary to know the decay scheme of Co^{60} in order to obtain Eqs. 73-75. It is possible, however, to determine simple decay schemes such as that of Co^{60} by means of a qualitative study of coincidence measurements such as the one described here.* Then, having determined the counter efficiencies, more complicated decay schemes may be studied.

B. Statistical Considerations

Since in practice the rate at which coincidences are recorded is very low, it is of great importance to consider the effect of statistical fluctuations on the results obtained. The true coincidence rate** may be deduced from the observed coincidence rate by means of Eqs. 66 and 70. If τ_c is determined experimentally, then the accidental coincidence rate N_a may be deduced from EQ. 70. Ordinarily the quantity τ_c is also calculated by means of Eq. 70. The counters,

*See, for example, the series of articles by Roberts and others (11-16).

**The term "true coincidence rate" is customarily employed to designate coincidences due to particles which are actually emitted in cascade, as opposed to the accidental coincidence rate.

C_1 and C_2, are actuated by separate sources and the three counting rates N'_o, N'_1 and N'_2 are determined, where the primes are used to indicate that these quantities refer to a resolving time determination. Since in this case there are no true coincidences,

$$N'_o = N'_a,$$

and thus

$$\tau_c = \frac{N'_o}{2N'_1 N'_2} . \tag{79}$$

Having determined τ_c by means of this experiment, the term N_a is calculated for the coincidence measurement in question. Then, from Eq. 66, the true coincidence rate is given by

$$N_c = N_o - N_a,$$

or, using Eq. 70, this becomes:

$$N_c = N_o - 2 \tau_c N_1 N_2. \tag{80}$$

It is evident from Eq. 80 that the true coincidence rate is determined from the measured quantities N_o, τ_c, N_1 and N_2. The standard deviation in N_c is then given by (Worthing and Geffner (31, p. 208)):

$$\sigma^2(N_c) = \left(\frac{\partial N_c}{\partial N_o}\right)^2 \sigma^2(N_o) + \left(\frac{\partial N_o}{\partial \tau_c}\right)^2 \sigma^2(\tau_c) + \left(\frac{\partial N_c}{\partial N_1}\right)^2 \sigma^2(N_1) + \left(\frac{\partial N_c}{\partial N_2}\right)^2 \sigma^2(N_2). \tag{81}$$

If Eq. 80 is used, Eq. 81 may be written in the form:

$$\sigma^2(N_c) = \sigma^2(N_o) + (2 \tau_c N_1 N_2)^2 \left[\frac{\sigma^2(\tau_c)}{\tau_c^2} + \frac{\sigma^2(N_1)}{N^2_1} + \frac{\sigma^2(N_2)}{N^2_2} \right]. \tag{82}$$

In a similar way the standard deviation in τ_c may be found to be given by:

$$\sigma^2(\tau_c) = \left(\frac{N'_o}{2N'_1N'_2}\right)^2 \left[\frac{\sigma^2(N'_o)}{N_o'^2} + \frac{\sigma^2(N'_1)}{N_1'^2} + \frac{\sigma^2(N'_2)}{N_2'^2}\right] \tag{83}$$

The standard deviation in any measured counting rate, due to random events, is given by (Rutherford, Chadwick and Ellis (32, p. 168)):

$$\sigma(N_i) = \sqrt{\frac{N_i}{t_i}} \quad , \tag{84}$$

where N_i is the counting rate concerned and t_i is the time of counting. Since radioactive decay is such a process; it is seen that in any particular measurement of a counting rate due to a radioactive source, the fractional standard deviation,

$$\frac{\sigma(N_i)}{N_i}$$

is given by

$$\frac{\sigma(N_i)}{N_i} = \frac{1}{\sqrt{N_i\, t_i}} \quad , \tag{85}$$

and is thus inversely proportional to the square root of the counting rate. If this fact is used, together with the fact that in any coincidence measurement with counters of ordinary efficiency, which is much less than unity, the coincidence rate is much less than the individual counting rates N_1 and N_2; then it is seen that the only important terms in Eqs. 82 and 83 are the terms involving

$$\sigma^2(N_o) \text{ and } \sigma^2(N'_o).$$

These equations may thus be written to a good approximation:

$$\sigma^2(N_c) = \sigma^2(N_o) + (2\ \tau_c\ N_1 N_2)^2 \quad \frac{\sigma^2(\tau_c)}{\tau_c^2}\ , \qquad (86)$$

$$\sigma^2(\tau_c) = \frac{\sigma^2(N'_o)}{(2\ N'_1\ N'_2)^2}\ . \qquad (87)$$

Two general procedures for determining τ_c may be mentioned. The customary procedure is to carry out a determination before and after the measurement of true coincidences, by means of the method outlined above. Very often the separate sources used to actuate the counters C_1 and C_2 are of such a strength that the counting rates N'_1 and N'_2 are high, resulting in a small error $\sigma(\tau_c)$. An alternative procedure is the continuous determination of τ_c, by alternating measurements of N'_o with measurements of N_o. Furthermore, the separate sources used in the determination of N'_o may be adjusted to such a strength that $N'_1 \cong N_1$ and $N'_2 \cong N_2$. If this is done, the effects of any variation of τ_c with time and with counting rate are minimized. This method must be considered the most reliable; although the time required to attain a given value for the measured standard deviation, $\sigma(N_c)$, may be considerably lengthened. In the work to be discussed below, the accidental coincidence rate, N_a, is of the order of the true coincidence rate, N_c; and consequently any error in the determination of τ_c may involve serious errors in the final results. For this reason the second method of determining τ_c has been employed. This method will now be discussed in greater detail.

Consider a particular coincidence measurement to be made with a source of strength N, and decay coefficients n_i and a_{ij}. From Eqs. 66, 69 and 70:

$$N_c = aN\ , \qquad (88)$$

$$N_a = bN^2\ , \qquad (89)$$

$$N_o = N_c + N_a \qquad (90)$$

$$= aN + bN^2, \qquad (91)$$

where

$$a = \sum_i \sum_j a_{ij}\ e_{1i}\ e_{2j} \qquad (92)$$

$$b = 2\ \tau_c \sum_i \sum_j n_i\ e_{1i}\ n_j\ e_{2j}. \qquad (93)$$

Thus a and b are functions of the type of source and of the experimental arrangement, but not of the source strength N, or of the time of counting. It is of interest to determine the optimum source strength to be selected and the optimum apportionment of counting time between the determination of N_o and of τ_c. Let:

$$x = aN \quad , \tag{94}$$

$$c = b/a^2. \tag{95}$$

Then Eqs. 88-90 become:

$$N_c = x \quad , \tag{96}$$

$$N_a = c\,x^2 \, , \tag{97}$$

$$N_o = x + c\,x^2. \tag{98}$$

The standard deviation in N_c is given by Eqs. 86 and 87:

$$\sigma^2(N_c) = \sigma^2(N_o) + \frac{(2\,N_1N_2)^2}{(2N'_1N'_2)^2}\,\sigma^2\,(N'_o),$$

and if in the determination of τ_c, $N'_1 \cong N_1$, and $N'_2 \cong N_2$, this becomes:

$$\sigma^2(N_c) \cong \sigma^2(N_o) + \sigma^2(N'_o).$$

If Eq. 85 is used, this becomes:

$$\sigma^2(N_c) = \frac{N_o}{t_o} + \frac{N'_o}{t_a} \quad ,$$

where t_o and t_a are the times of counting N_o and N'_o. Since $N'_o \cong N_a$, this becomes:

$$\sigma^2(N_c) \doteq \frac{N_o}{t_o} + \frac{N_a}{t_a} \, .$$

From Eqs. 96-98, this may be written:

$$R^2 = \frac{1 + cx}{t_o x} + \frac{c}{t_a} \quad , \tag{99}$$

where

$$R = \frac{\sigma(N_c)}{N_c}$$

is the fractional standard deviation in the true coincidence rate, N_c. If the total time of counting is T, then Eq. 99 may be written:

$$R^2 = \frac{1 + cx}{t_o x} + \frac{c}{T - t_o} . \qquad (99a)$$

The apportionment of the total time T between t_o and t_a which will give the lowest possible value for R is obtained by setting the derivative of R with respect to t_o equal to zero. This results in the relation:

$$\frac{t_a}{t_o} = \sqrt{\frac{cx}{1 + cx}} = \sqrt{\frac{N_a}{N_o}} . \qquad (100)$$

This gives the relative amount of time to be taken in determining τ_c and N_o. It is of interest next to determine the proper source strength N to be employed. This is equivalent to determining the proper value of x. It is seen by inspection of Eq. 99a that there is no minimum of R with respect to x. The larger x is made, the smaller will R become. If t_a and t_o are eliminated from Eq. 99 by means of Eq. 100, the result is:

$$R = \frac{c}{T} F(y), \qquad (101)$$

where

$$y = cx = N_a/N_c \qquad (102)$$

and

$$F(y) = \left[\left(1 + \sqrt{\frac{y}{1 + y}}\right)\left(\frac{1 + y}{y} + \sqrt{\frac{1 + y}{y}}\right)\right]^{1/2} \qquad (103)$$

The value of the function F(y) is tabulated in Table I for four points of interest.

Table I

The Function F(y)

y	F(y)
0	∞
1	2.42
2	2.22
∞	2.00

It is seen that R is reduced by only about 20% or less by selecting y greater than unity. Thus a reasonable value for y is given by $y \cong 1$, or

$$N_a = N_c \ . \tag{104}$$

Thus the statistical error in determining the coincidence rate N_c is given by

$$\frac{\sigma(N_c)}{N_c} = 2.42 \sqrt{\frac{c}{T}}$$

$$= 2.42 \sqrt{\frac{b}{a^2 T}} \ , \tag{105}$$

with the source strength chosen such that $N_c = N_a$, and with

$$\frac{t_a}{t_o} = \sqrt{\frac{N_a}{N_o}} = .707.$$

If the factors a and b are evaluated from Eqs. 92 and 93, then Eq. 105 becomes:

$$\frac{\sigma(N_c)}{N_c} = 3.42 \left[\frac{\tau_c \sum_i \sum_j n_i \, n_j \, e_{1i} \, e_{2j}}{T(\sum_i \sum_j a_{ij} \, e_{1i} \, e_{2j})^2} \right]^{1/2} . \tag{106}$$

Thus it is seen that the fractional error in N_c varies directly as the square root of τ_c and inversely as the square root of the counter efficiencies e_{1i} and e_{2j}. It is thus of importance to maintain τ_c as small as possible without losing true coincidences, and to maintain the counter efficiencies as large as possible.

A limitation which has not been considered in the above analysis is the possibility of loss of counts in the individual counters due to the dead time of the counters. If it is desired to avoid excessive loss in the counters it may be necessary either to reduce the source strength below that given by Eq. 104, or to reduce the counter efficiencies e_{1i} and e_{2j} by decreasing the solid angles. The effect of either of these alternatives may be investigated in any particular case by use of Eq. 104. In general it is found to be preferable to reduce the source strength until the counting loss in the individual counters is not excessive.

Another effect which has not been treated above is the presence of backgrounds due to cosmic radiation and stray contamination. The source strengths used in the measurements to be described are ordinarily sufficiently great that these effects are not of interest in the problems considered above.

C. Coincidence Measurements with the Beta-Ray Spectrometer

The spectrometer used in this investigation has been described by Jensen (3). A schematic diagram of the spectrometer is shown in Fig. 3. The spectrometer counter, which will be designated hereafter as C_1, is inserted into the spectrometer at the end opposite to the source, as shown in Fig. 3. Immediately behind the source is inserted the secondary counter which will be designated as C_2. C_1 and C_2 are connected electrically with the coincidence circuit and individual registers as shown in Fig. 12. The coincidence circuit used is a modification of that of Moak (33). Pulses from C_1 and C_2 are introduced into separate channels of this coincidence circuit, where they are used to trigger standard square wave pulses of 5 microseconds duration. These standard pulses are fed to a Rossi type coincidence stage, which registers coincidences on a mechanical register. In addition they are fed to separate output stages which are connected to Los Alamos type Mod. 200 scalers*, which record

*For a description of these scalers, see the paper by Gallagher, Higinbotham and Sands (34).

the individual counting rates in C_1 and C_2. The coincidence resolving time τ_c may be varied in six steps from 0.5 microseconds to 3 microseconds. A comparison of observed coincidence rates at different setting of τ_c, with the Geiger counters used in the experiments described below, indicated that coincidences began to be lost, due to lags in the time of firing of the counters, at resolving times less than one microsecond. For this reason, no resolving time less than one microsecond was used in any of the experiment described below.

When coincidences were to be counted in the spectrometer, the source was mounted on a thin film of aluminum or mica which was in turn mounted on a lucite wafer. This wafer was then attached to the 2 inch diameter brass source tube which fits into the source end of the spectrometer tube. C_2 was then inserted into this tube behind the source. In the case where C_2 was a gamma-counter, the source tube was sealed behind the source with a 10 mil phosphor bronze (0.241 g./cm^2) foil, so that the gamma-counter could be removed without destroying the vacuum in the spectrometer tube. In the case where C_2 was a beta-counter, such a foil was not permissible, and it was necessary to provide the beta-counter with a vacuum seal to prevent leakage of air between the outer wall of the counter and the inner wall of the source tube. In Fig. 14 are shown schematic diagrams of the beta- and gamma-counter assemblies.

The gamma-counter was made from a copper cylinder, the interior of which was 1.5 inches in diameter and 6 inches in length. Within this cylinder was inserted a lining of 80-mesh platinum gauze which covered the wall and the face of the counter nearest to the source. The gamma-counter with the gauze lining was found to have an efficiency 1.4 times as great at 1.25 Mev as a similar counter without the gauze, and 4.2 times as great at 0.4 Mev. The counter was provided with a 2 mil brass (0.0422 g/cm^2) window. The beta-counter was a commercial end-window counter with a steel wall and a 2.5 mg/cm^2 mica window. This counter was mounted within an aluminum cylinder with dimensions similar to those of the gamma-counter. The gamma-counter subtended a solid angle at the source of 10%, and the beta-counter subtended a solid angle of 2%.

It will be of interest to make some rough calculations to determine the feasibility of making coincidence measurements in the spectrometer with the arrangement described here.

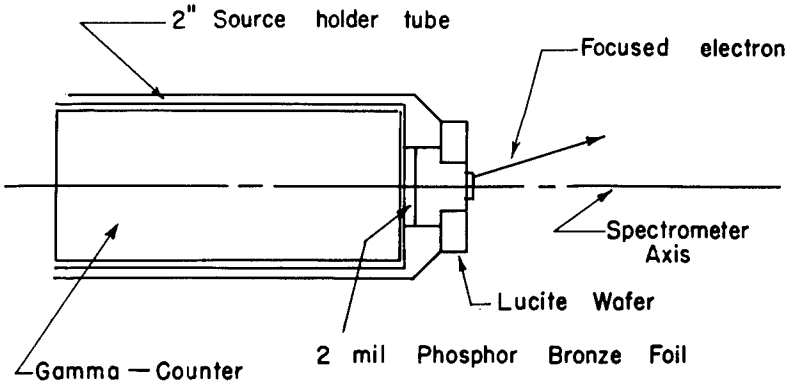

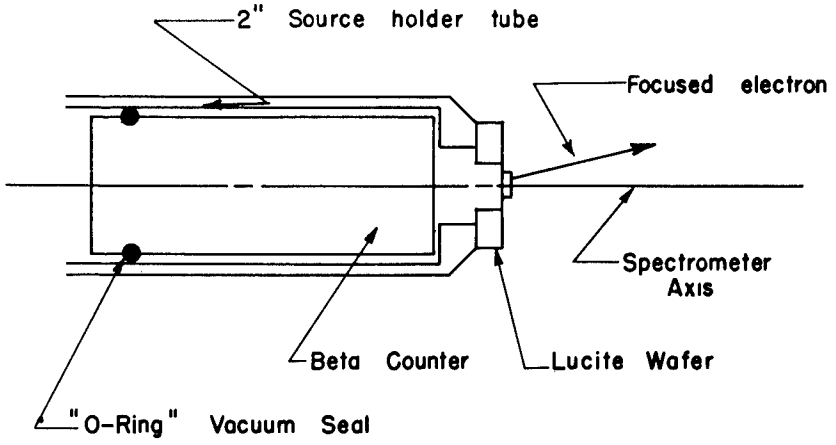

Fig. 14--Gamma-counter and beta-counter assemblies for coincidence measurements in the spectrometer.

Consider first a coincidence measurement in which two gamma-rays are in cascade. Let one of these gamma-rays be completely converted in the K shell, and let the other be converted only to a negligible degree. Let the focusing current of the spectrometer be adjusted to focus the conversion electrons. Then:

$$N_1 = N\, e_s, \tag{107}$$

$$N_2 = N\, e_\gamma\,. \tag{108}$$

$$N_c = N\, e_s\, e_\gamma, \tag{109}$$

$$N_a = 2\ \tau_c\, N_1\, N_2 = 2\ \tau_c\, e_s\, e_\gamma\ N^2. \tag{110}$$

Since τ_c is to be as low as possible without losing true coincidences, it may be taken as 10^{-6} sec. The efficiency of a Geiger counter for gamma-radiation, including the effect of a 10% solid angle, may be taken as of the order of 10^{-3} (Von Droste (30)). The efficiency of the spectrometer for internal conversion electrons is obtained from Eq. 60:

$$e_s = \omega e_c\, S(\alpha).$$

If the source is sufficiently thin, and the electron energy sufficiently high, then $S(\alpha)$ and e_c may be taken as unity. Since ω is of the order of 1%,

$$E_s \cong 10^{-2}.$$

In order to minimize the statistical error it is desirable to choose a source strength such that $N_c \cong N_a$ (Eq. 104). If this is done, and if the proper apportionment of counting times, as given by Eq. 100, is used then from Eq. 105:

$$\frac{\sigma(N_c)}{N_c} = 2.42 \sqrt{\frac{b}{a^2 T}}\ . \tag{111}$$

Comparing Eqs. 109 and 110 with Eqs. 88 and 89, it is seen that:

$$a = e_s\, e_\gamma = 10^{-5}$$

$$b = 2\ \tau_c\, e_s\, e_\gamma = 2 \times 10^{-11}.$$

Inserting these values in Eq. 111 leads to the result:

$$\frac{\sigma(N_c)}{N_c} = \frac{1}{\sqrt{T(\text{sec.})}} \qquad (112)$$

It will thus take a very short time to attain a low statistical error, and the experiment may be considered feasible. It must be observed that when the source strength is chosen such that $N_c = N_a$, the counting rate N_1 is found to be of the order of 500 counts per sec. With a counter dead time of the order of 2×10^{-4} sec., this will result in a counting loss of 10% in C_1. For this reason it would be desirable to choose a somewhat weaker source that that implied by Eq. 104.

As another example, consider the case where neither of the gamma-rays is converted. In order to perform a measurement in the spectrometer, it will then be necessary to use a radiating foil, and count Compton electrons or photoelectrons emitted from the foil by the gamma-ray. The efficiency of the spectrometer in the case of photoelectrons is given by Eq. 62:

$$e_s = \omega e_c S(\alpha)(\tau X).$$

Since $\tau \cdot X$ is customarily of the order of 10^{-3}, the term e_s is of the order of 10^{-5}. Replacing e_s in the previous case by 10^{-5} leads to the result:

$$\frac{\sigma(N_c)}{N_c} = \sqrt{\frac{10^3}{T(\text{sec.})}} \qquad (113)$$

For an error in N_c of 10%, this requires a counting time of 28 hours. Such an experiment must be regarded as possible, but not particularly promising.

Other cases may be treated in a similar manner and need not be discussed here.

D. Determination of Counter Efficiencies

As the first example of a coincidence measurement in

the spectrometer, the determination of the spectrometer solid angle ω, and of the gamma-counter efficiency at 1.25 Mev will be discussed. A thin source of Co^{60} was inserted in the source position of the spectrometer. A brass plug of surface density 3.97 g/cm^2 was inserted in front of the gamma-counter to provide shielding against electrons. The counting rates to be expected under these conditions are deduced from the known decay scheme of Co^{60} (Fig. 13):

$$N_1 = N\, e_s(\beta), \tag{114}$$

$$N_2 = N\, [\bar{e}_\gamma(1.1 \text{ Mev}) + e_\gamma(1.3 \text{ Mev})], \tag{115}$$

$$N_c = N\, e_s(\beta)\, [\bar{e}_\gamma(1.1 \text{ Mev}) + e_\gamma(1.3 \text{ Mev})]. \tag{116}$$

The term $e_s(\beta)$ is given by Eq. 61:

$$e_s(\beta) = \frac{\omega\, e_c(p_o)\, h\, p_o\, n(p_o)}{\int_o^\infty n(p_o)\, d\, p_o} \equiv \omega A,$$

where

$$A \equiv \frac{e_c(p_o)\, h\, p_o\, n(p_o)}{\int_o^\infty n(p_o)\, d\, p_o}.$$

The factor A was evaluated by measuring the spectrometer transmission curve and the calibration constant K, using the ThB - F line; and the shape of the beta-spectrum of Co^{60}, extrapolating below the low energy cutoff of the spectrometer counter by means of the theoretical Fermi distribution as given by Feister (35). The result was

$$A = 0.0485.$$

The half-width of the spectrometer transmission curve was found to be

$$h = 0.049.$$

Since the efficiency of a Geiger counter for detecting gamma-radiation is a slowly varying function of energy, Eqs. 114-116 may be written approximately:

$$N_1 = N A \omega = 0.0485 N \omega ,$$

$$N_2 = 2 N e_\gamma (1.25 \text{ Mev}),$$

$$N_c = 2 N A \omega e_\gamma (1.25 \text{ Mev})$$

$$= .096 N \omega e_\gamma (1,25 \text{ Mev}).$$

The measured values, after correcting for accidental coincidences and backgrounds, were*;

$$N_1 = 531 \text{ counts per min},$$

$$N_2 = 4649 \text{ counts per min},$$

$$N_c = 0.815 \pm 0.079 \text{ counts per min}.$$

From these relations, and Eqs. 114-116, there results:

$$e_\gamma(1.25 \text{ Mev}) = (0.767 \pm 0.074) \times 10^{-3},$$

$$\omega = (0.362 \pm 0.035) \times 10^{-2},$$

$$N = (3.03 \pm 0.29) \times 10^6 \text{ dis. per min},$$

$$= 1.36 \pm 0.13 \text{ microcuries}.$$

A repetition of this experiment led to the results:

$$e_\gamma(1.25 \text{ Mev}) = (0.688 \pm 0.069) \times 10^{-3},$$

$$\omega = (0.340 \pm 0.034) \times 10^{-2},$$

$$N = 1.52 \pm 0.15 \text{ microcuries}.$$

When these values are averaged, there results for the efficiency of the gamma-counter at 1.25 Mev, and for the efficiency of the spectrometer for monoenergetic electrons:

$$e_\gamma = (0.728 \pm 0.051) \times 10^{-3},$$
$$\omega = (0.351 \pm 0.024) \times 10^{-2}.$$

---

*Errors (±) given in this paper will refer to standard deviation.

This value for e_γ, applies only when the gamma-counter is used with the 3.97 g/cm^2 brass plug. It will be of more general interest to correct this value to refer to the extrapolated efficiency with no absorbing material between the source and the interior of the gamma-counter. It will thus be necessary to correct for absorption in the brass plug, in the brass counter window, and in the phosphor bronze foil attached to the end of the source holder. The absorption coefficient of brass is taken to be the same as that of copper. The absorption coefficient of phosphor bronze is taken to be that of a mixture of 80% copper and 20% tin (Handbook of Chemistry and Physics (36, p. 1201)). Absorption coefficients are taken from data of Heitler (24, p. 160), Hulme and others (37), and Compton and Allison (38, p. 800-806). When this correction is made, the result for the extrapolated efficiency of the gamma-counter is

$$e_\gamma^{\circ}(1.25 \text{ Mev}) = (0.90 \pm 0.06) \times 10^{-3} ,$$

where the superscript ($^\circ$) refers to the extrapolated efficiency.

Since the efficiency of a gamma-counter is in general a function of energy, it is necessary to determine the efficiency for several energy values in order to have a useful method of interpreting data. The efficiency of the gamma-counter at two other points may be obtained by means of a coincidence measurement using ThB.

The transition ThB → ThC has recently been studied by Martin and Richardson (39), and by Feather, Kyles and Pringle (19). The decay scheme is indicated in Fig. 15. From the data of these authors, the number of internal conversion K electrons per disintegration (α_K) corresponding to the gamma-ray may be determined.

From the data of Martin and Richardson (39):

$$\alpha_K = 0.332.$$

From the data of Feather, Kyles and Pringle (19):

$$\alpha_K = 0.228.$$

The average of these two values is:

$$\alpha_K = 0.31.$$

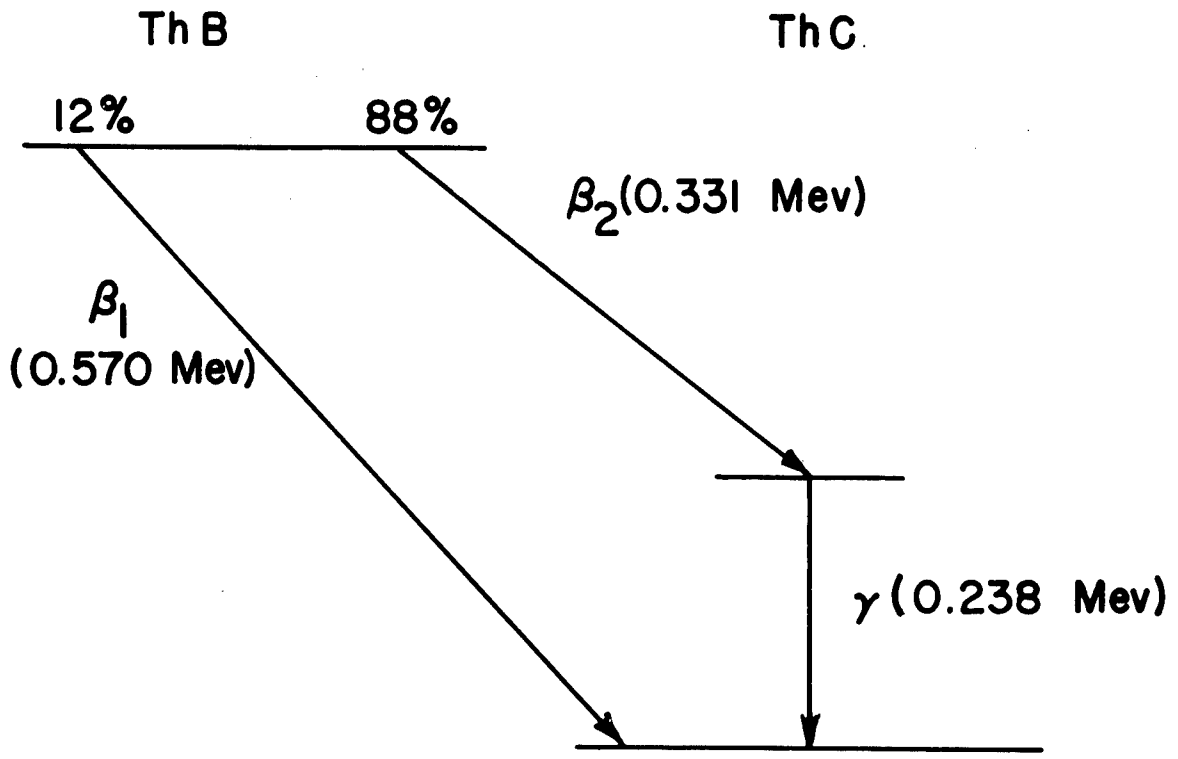

Fig. 15--Decay scheme of ThB→ThC.

If the number of L-converted electrons per disintegration (α_L) is given by*:

$$\frac{\alpha_L}{\alpha_K} = \frac{15}{115}, \qquad \alpha_L = 0.04,$$

and if α_M, α_N, etc. are neglected, then the number of gamma-quanta per disintegration is given by

$$\gamma = 0.88 - (0.31 + 0.04) = 0.53.$$

The electron spectrum of ThB is such that in the vicinity of the K conversion line (ThB - F line) the only significant contribution of the beta-spectrum is due to β_2, which is in coincidence with the gamma-ray. Now let the spectrometer be set to focus electrons due to the ThB - F line, which is superimposed on the spectrum of β_2. The spectrometer counting rate will be given by:

$$N_1 = 0.31\ N\ e_s + 0.88\ A\ N\ \omega .$$

There will be coincidences between the internal conversion electrons of the F line and their associate 0.090 Mev X-rays, between the beta-rays and these X-rays, and between the beta-rays and the 0.238 Mev gamma-rays. The resulting coincidence rate is then given by:

$$N_c = 0.31\ N\omega P e_\gamma(0.090\ \text{Mev}) + N\omega\,[0.31\ P e_\gamma(0.090\ \text{Mev}) + 0.53\ e_\gamma(0.238\ \text{Mev})],$$

where ω is used for e_s(IC) since the source is very thin, and where P is the fluorescence yield for the ThC-X-rays.

Now let the spectrometer focusing current be decreased slighly, so that the F line is no longer focused. Then the counting rates become:

$$N_1' = 0.88\ A\ N\ \omega ,$$

$$N_c' = A\ N\ \omega\,[0.53\ e_\gamma\ (0.238\ \text{Mev}) + 0.31\ P\ e_\gamma\ (0.090\ \text{Mev})] .$$

---

*For information concerning conversion coefficients in the naturally radioactive elements, see Rasetti (40, p. 134).

Thus:

$$\frac{N_c - N_c'}{N_1 - N_1'} = P\, e_\gamma\,(.090 \text{ Mev}), \qquad (117)$$

and

$$\frac{N_c'}{N_1'} = \frac{0.53\, e_\gamma(0.238 \text{ Mev}) + 0.31\, P\, e_\gamma\,(0.090 \text{ Mev})}{0.88} \qquad (118)$$

From Eqs. 117 and 118, if P is known, the efficiency of the gamma counter at 0.090 Mev and 0.238 Mev may be determined from the coincidence experiments described. Although the fluorescence yield P is not known exactly, it may be deduced to be of the order of 0.9, by extrapolation of the known values of P (Compton and Allison (38, p. 488)). A coincidence experiment such as that described above led to the following results:

$$e_\gamma^{\,o}\,(0.090 \text{ Mev}) = (0.55 \pm 0.10) \times 10^{-3},$$

$$e_\gamma^{\,o}\,(0.238 \text{ Mev}) = (0.85 \pm 0.15) \times 10^{-3},$$

where the efficiencies extrapolated to zero thickness of material between source and counter interior are given. Using these values, together with the previously determined value at 1.25 Mev, a curve of e_γ as a function of gamma-ray energy is plotted in Fig. 16. Also plotted in Fig. 16, is a curve indicating the variation of efficiency of a platinum gamma-counter as calculated by the method of Von Droste (30). The calculated efficiency curve is normalized arbitrarily, since the effective solid angle subtended by the counter is not known.

E. Decay Scheme of Hf^{181}

The 46 day activity due to Hf^{181} has been studied by many investigators (41-50, 52). The decay scheme most generally accepted until recently was that originally proposed by Chu and Wiedenbeck (41) and indicated in Fig. 17. It has recently been suggested by Deutsch and Hedgran (52)

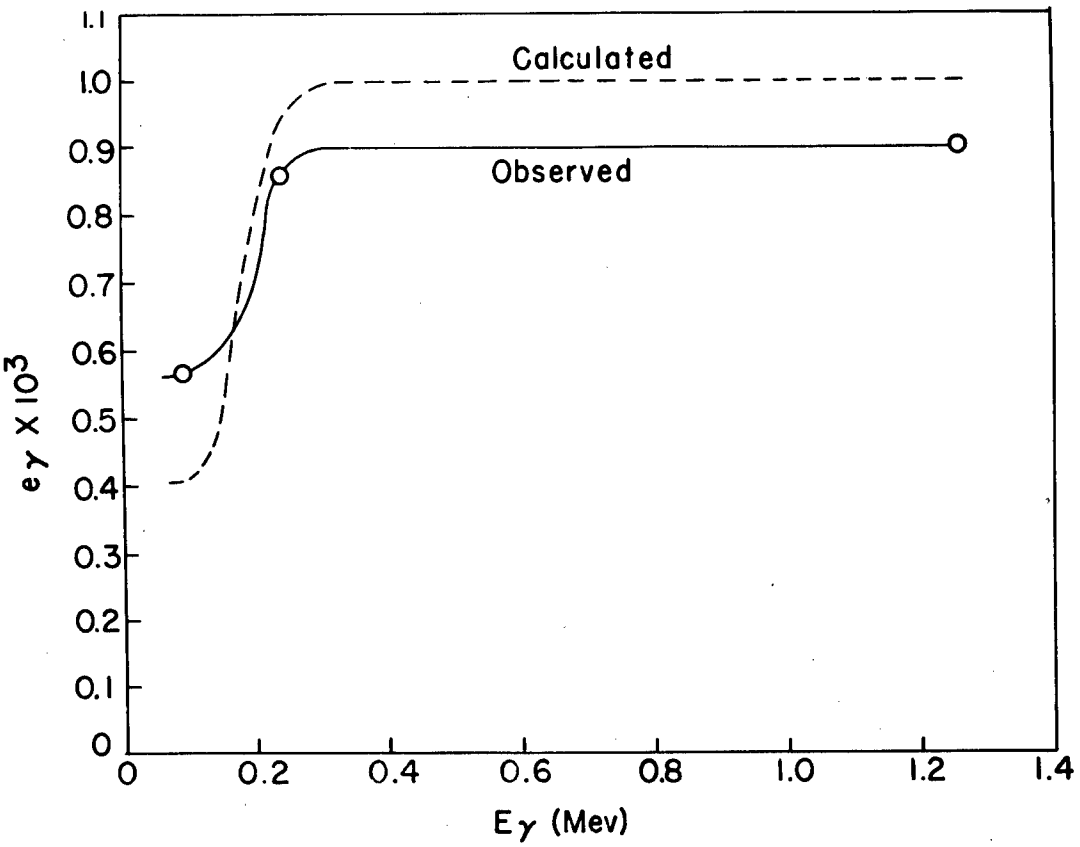

Fig. 16--Efficiency of platinum grid gamma-counter.

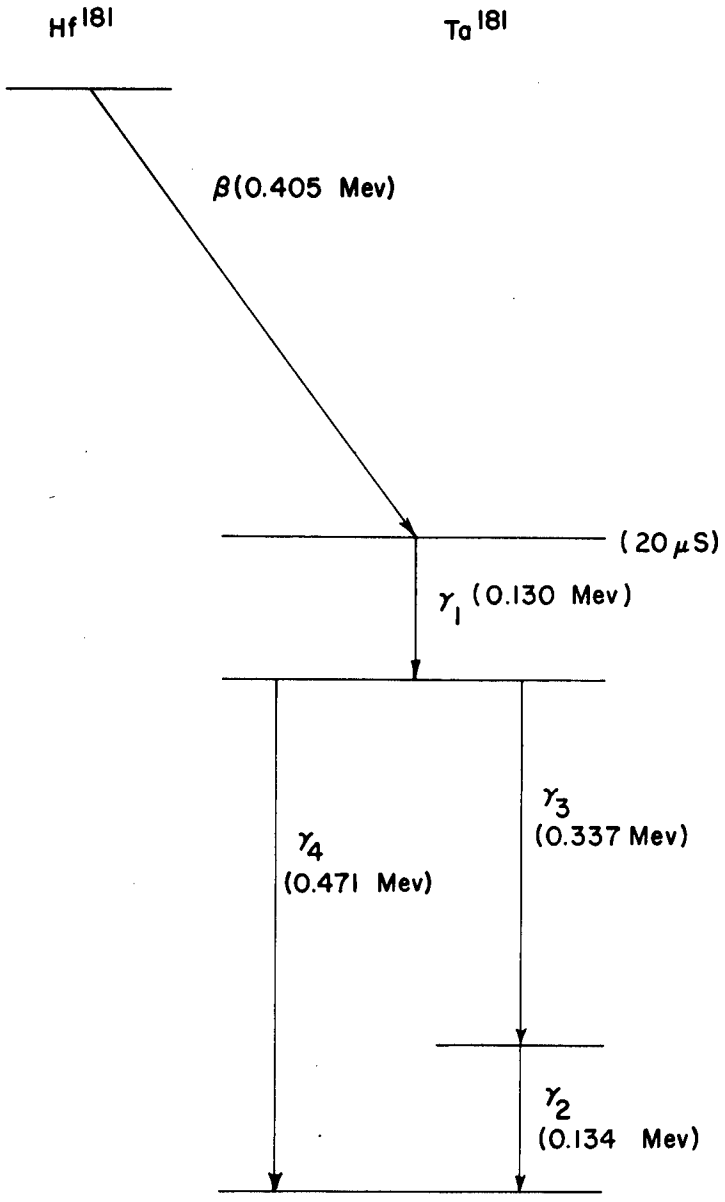

Fig. 17--Decay scheme of Hf^{181} proposed by Chu and Wiedenbeck.

that this decay scheme cannot be correct, since these authors find the transition corresponding to γ_3 to be associated with a longer-lived activity than Hf^{181}. It will be the purpose of the investigation described here to use the coincidence method to analyze the decay scheme of Hf^{181}.

Analysis of the coincidence data assuming the decay scheme of Chu and Wiedenbeck: Let it be assumed first that the decay scheme of Chu and Wiedenbeck is correct, with the exception of possible rearrangements of the order of the various transitions.

In Table II are given the conversion probabilities of internal conversion electrons due to the various gamma-rays. These probabilities designated by α_{1K}, α_{1L}, etc. are the values measured by Chu and Wiedenbeck (41) and are defined as the number of electrons per decaying atoms of Hf^{181}.

Table II

Hf^{181} Conversion Probabilities

Line	Conversion Prob.	Line	Conversion Prob.
α_{1K}	0.56	α_{3K}	0.019
α_{2K}	0.22	α_{3L}	0.0053
$\alpha_{1L} + \alpha_{2L}$	0.425	α_{4K}	0.021
$\alpha_{1M} + \alpha_{2M}$	0.089	α_{4L}	0.0071

In addition to the conversion probabilities listed in Table II, Chu and Widenbeck (41) have measured the ratio of gamma-ray intensities of γ_3 and γ_4 by two methods. Using a lead radiator in a beta-ray spectrometer, they obtained both Compton distributions and photoelectron peaks. Comparison of the Compton distributions gives a ratio of intensities of γ_3 to γ_4 of 1:2. Comparison of the photoelectron peaks gives a ratio of 1:2.8. For the purpose of the present investigation, the average of these two values will be used. The result for the ratio of the quantum intensities of γ_3 to γ_4 is then 0.428.

From the above information, it is possible to deduce the relative number of each type of transition within fairly narrow limits. Let γ_i represent the number of quanta of type i per decaying atom of Hf^{181}, and let T_i represent the total number of transitions of type i per decaying atom. Thus

$$T_i = \gamma_i + \alpha_{iK} + \alpha_{iL} + \alpha_{iM} + \ldots .$$

The following relations may then be deduced:

$$T_1 = 1, \qquad T_2 = T_3 = 0.306, \qquad T_4 = 0.694$$

$$\gamma_1 = \alpha_{2L} + \alpha_{2M} - 0.074$$

$$\gamma_2 = \alpha_{1L} + \alpha_{1M} - 0.428$$

$$\gamma_3 = 0.282 \qquad \gamma_4 = 0.666$$

$$\alpha_{1L} + \alpha_{2L} = 0.425$$

$$\alpha_{1M} + \alpha_{2M} = 0.089 .$$

The only undetermined quantities are α_{1L}, α_{2L}, α_{1M}, α_{2M} and consequently γ_1 and γ_2. Although there is not sufficient information available to determine these quantities uniquely, it is possible to obtain approximate values by considering two limiting cases:

Case I: The probability α_{1L} is as large as possible. There results:

$$\alpha_{1L} = 0.425 \qquad \alpha_{2L} = 0$$

$$\alpha_{1M} \cong 0.009 \qquad \alpha_{2M} \cong 0.08$$

$$\gamma_1 \cong 0.006 \qquad \gamma_2 \cong 0.006$$

Case II: The probability α_{2L} is as large as possible. There results:

$\alpha_{1L} = 0.339$ $\quad\quad$ $\alpha_{2L} = 0.086$

$\alpha_{1M} = 0.089$ $\quad\quad$ $\alpha_{2M} = 0$

$\gamma_1 = 0.012$ $\quad\quad$ $\gamma_2 = 0$.

These two extreme cases do not lead to very different results when used to predict the data to be expected from spectrometer coincidence measurements. For the purpose of the present investigation, Case I will be assumed. The decay scheme indicated in Fig. 18 results from Case I.

The results of the first set of coincidence measurements are indicated in Table III. These measurements were made with the spectrometer operating at a half-width of 4.9% and a solid angle ω of 0.35%. Due to the thickness of the Hf^{181} source used, the spectrometer efficiency was reduced by a factor of approximately 3 when focusing on the conversion line α_{1L}. Thus $S(\alpha) \cong 1/3$ (Eq. 64). Furthermore since a large window (2.2 cm diam) counter was used as the spectrometer counter, and a correspondingly thick window was required, the counter efficiency e_c was considerably reduced for energies corresponding to the conversion line α_{1K}. For this reason, no coincidence measurements were made with the spectrometer focused on the line α_{1K}. The platinum grid gamma-counter was used as C_2. The total thickness of material between the source and the gamma-counter interior was 0.241 g/cm^2 of phosphor bronze and 0.0422 g/cm^2 of brass.

Column 1 in Table III indicates the code number of the experiment. Column 2 indicates the part of the Hf^{181} electron spectrum on which the spectrometer was focused. Column 3 indicates the coincidence counting rate, corrected for coincidences due to the beta-spectrum in cases where the spectrometer was focused on a conversion line superimposed on this spectrum. Columns 4 and 5 indicate the ratio of the coincidence rate to the counting rates in the gamma-counter and in the spectrometer respectively. The counting rate in the spectrometer, N_1, was corrected where necessary for contributions due to the beta-spectrum on which a focused conversion line was superimposed. Column 5 indicates the ratio N_c/N_1 calculated on the basis of the decay scheme of Fig. 18. These calculations were performed in the same manner as in the determinations of counter efficiency previously discussed. The gamma-counter efficiency, as determined from Fig. 16, with corrections for absorption,

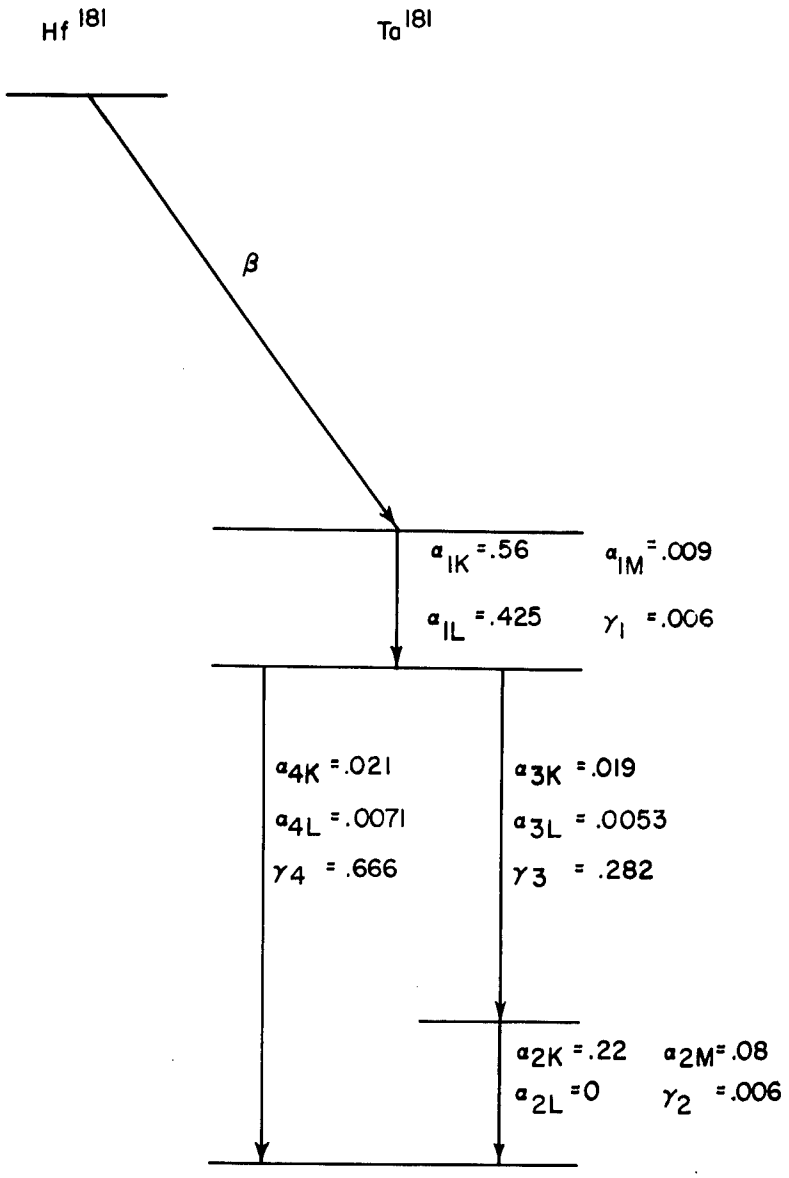

Fig. 18--Proposed decay scheme of Hf^{181} with conversion probabilities and gamma-ray intensities deduced from the data of Chu and Wiedenbeck.

Table III

Electron - Gamma Coincidence Measurements with Hf^{181}

Expt. No.	Spectral Component	N_c c/m	N_c/N_2 x 10^3	N_c/N_1 x 10^3	N_c/N_1 (Calc) x 10^3	τ_c μs	Delay
1	α_{1L}	1.39 ± 0.14	0.214 ± 0.022	0.795 ± 0.080	0.88	1.5	0
2	α_{3K}	0.192 ± 0.045	0.038 ± 0.009	0.83 ± 0.19	0.44	1.5	0
3	α_{4K}	0.197 ± 0.030	0.030 ± 0.005	0.71 ± 0.11	0.30	1.5	0
4	β	0.164 ± 0.058	0.030 0.010	0.24 ± 0.08	0.10	3	0
5	α_{1L}	0.112 ± 0.140	0.019 ± 0.023	0.068 ± 0.085	0	3	6 μs in C_1
6	β	0.062 ± 0.055	0.011 ± 0.010	0.089 ± 0.079	0.17	3	6 μs in C_1
7	α_{1L}	0 ± 0.12	0 ± 0.02	0 ± 0.07	0	3	6 μs in C_2

was used in these calculations. Due to the fact that the ratio N_c/N_1 does not depend on the spectrometer efficiency e_s, it was unnecessary to evaluate e_s. Columns 6 and 7 indicate respectively the resolving time τ_c and any delay introduced into either counting circuit.

Consider first the experiments in which the spectrometer was focused on the conversion line α_{1L}. It is seen that in experiment 1 the agreement between the calculated and observed ratio N_c/N_1 is fairly good. In experiments 5 and 7, delayed coincidences between γ_1 and the other gamma-radiation were sought. It is seen that no such coincidences were observed. Since it appears certain that the 20 microsecond metastable state is the initial state of the transition represented by γ_1, the above results rule out the possibility that this transition is preceded by γ_2, γ_3 and γ_4.

Further verification of this is furnished by the measurement in which the spectrometer was focused on the beta-spectrum alone. Measurements were made both with no delay and with a 6 microsecond delay in the spectrometer counter circuit. The observed ratios were:

$$N_c/N_1 = (0.24 \pm 0.08) \times 10^{-3}, \text{ no delay}$$

$$= (0.09 \pm 0.08) \times 10^{-3}, \text{ with delay.}$$

If the decay scheme of Fig. 18 is assumed, the calculated ratios are:

$$N_c/N_1 = 0.10, \text{ no delay}$$

$$= 0.17 \text{ with delay.}$$

On the other hand, if the metastable state is preceded by γ_2, γ_3 and γ_4, then the calculated ratios are:

$$N_c/N_1 = 1.0, \quad \text{no delay}$$

$$= 0, \quad \text{with delay.}$$

Although the observed coincidence rate was so low that the statistics are poor, the measurements are in better agreement with the decay scheme shown in Fig. 18 than with the alternative possibility.

When the spectrometer was focused on the conversion lines α_{3K} and α_{4K}, no interpretable results were obtained. The results from experiments 2 and 3 were:

α_{3K}: N_c/N_1(observed) = $(0.83 \pm 0.19) \times 10^{-3}$

N_c/N_1(calculated) = 0.44×10^{-3}

α_{4K}: N_c/N_1(observed) = $(0.71 \pm 0.11) \times 10^{-3}$

N_c/N_1(calculated) = 0.30×10^{-3}.

The observed coincidence rates are higher than the calculated values by a factor of 2. No explanation of these discrepancies is known. Although results of the observed order of magnitude might be expected if γ_3 and γ_4 were in cascade, the relative intensity measurements referred to above make it difficult to imagine any decay scheme in which this might be the case. A search for low energy gamma-radiation at energies as low as 0.01 Mev led to negative results. The possibility of coincidences due to bremsstrahlung has been considered. Calculations based on the bremsstrahlung cross section given by Heitler (24, p. 173) indicated that such coincidences should be negligible compared to the observed coincidence rate. An experimental test of this conclusion was made by shielding the source from the gamma-counter by means of an aluminum plate of sufficient thickness to stop all electrons. The coincidence rate remained essentially unchanged. The effect of internal bremsstrahlung (Chang and Falkoff (51)) has also been considered. A rough calculation of the magnitude of this effect indicated that it should be negligible. An experimental test of this conclusion was attempted using a Sr^{90} - Y^{90} pure beta-ray source. The experimental ratio N_c/N_1 was found to be $(0.02 \pm 0.3) \times 10^{-3}$. This result, due to the large error, is not conclusive but does appear to indicate a low coincidence rate.

The results of an absorption measurement are shown in Fig. 19. The spectrometer was focused on the conversion line α_{1L}, and electron-gamma-ray coincidences were observed as a function of the thickness of lead absorber between the source and the gamma-counter. The ratio N_c/N_2, normalized to unity at zero absorber thickness is indicated in Fig. 19, as a function of the absorber thickness. Also indicated in this figure are curves representing the behavior to be expected if γ_1 is in coincidence with (a) both γ_3 and γ_4, (b) γ_4 only, and (c) γ_3 only. The latter possibility is clearly ruled out by the observed data. Although the data

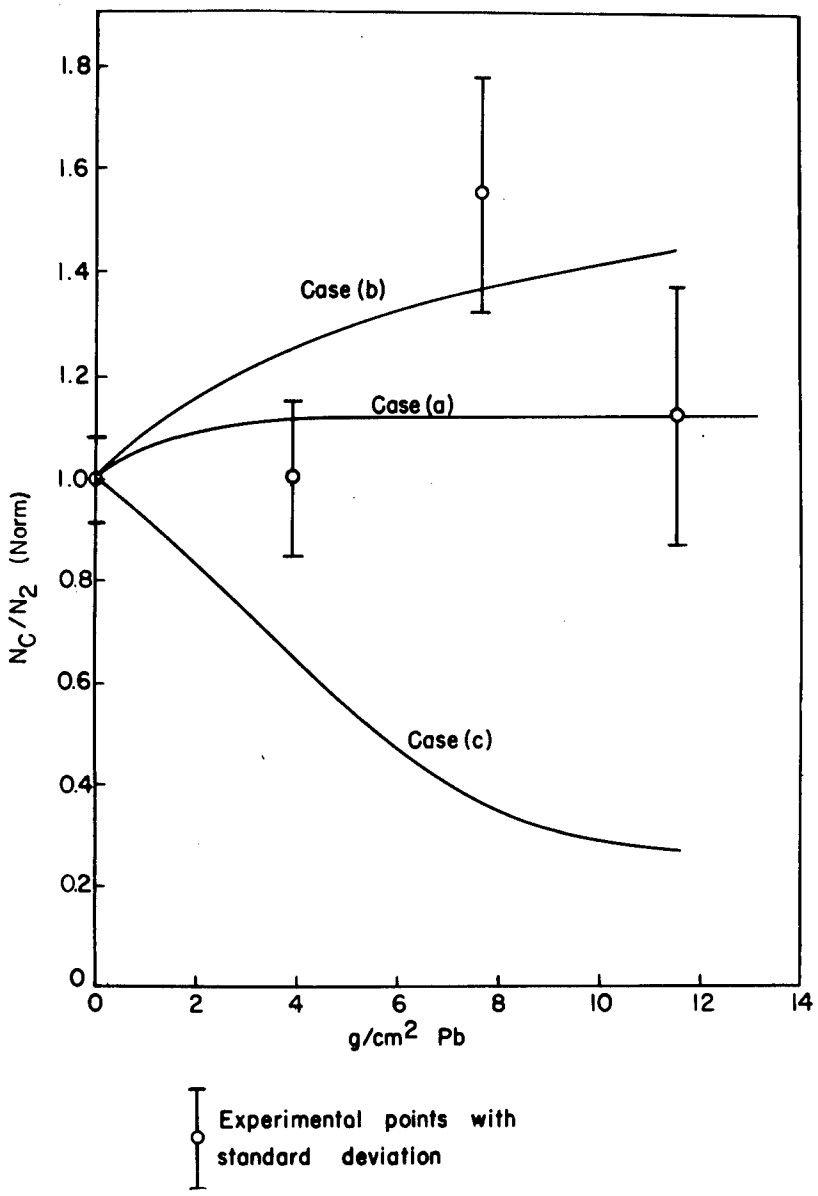

Fig. 19--Electron-gamma coincidence absorption measurement with Hf^{181}. The curves a, b, and c represent calculated absorption curves.

are not sufficiently precise to distinguish definitely between the first two cases, the agreement with case (a) is somewhat better than with case (b).

The results of the next set of coincidence measurements are indicated in Table IV. The spectrometer was again adjusted for a half-width of 4.9% and a solid angle of 0.35%. The end-window beta-counter was used as C_2. The mica window thickness of the counter and the mica backing of the source resulted in a total thickness of mica of 5 mg/cm^2 between the source and the interior of the beta-counter, C_2. Column 1 in Table IV indicates the code number of the experiment, and column 2 indicates the region of the Hf^{181} electron spectrum on which the spectrometer was focused. Column 3 indicates the observed coincidence rate, and columns 4 and 5 indicate the observed and calculated ratios N_c/N_1. Both N_c and N_1 were corrected for contributions due to the beta-spectrum on which the internal conversion lines are superimposed. Column 6 indicates the geometric solid angle subtended by C_2; column 7 indicates the resolving time τ_c, and column 8 indicates the thickness of any absorbing material between the source and the interior of C_2. Column 9 indicates any delay introduced into either counter circuit. The calculated ratios N_c/N_1 were computed in the same way as for the case of electron-gamma-ray coincidences. In this case, however, it was necessary to know the efficiency of the beta-counter in place of that of the gamma-counter used previously. This efficiency was assumed to be given by the product of the solid angle subtended at the source and of the transmission of electrons in the material between the source and the interior of the beta-counter, C_2. The transmission was obtained by measuring the spectrum of Compton electrons from Co^{60} in the spectrometer, using various thicknesses of window material in front of the spectrometer counter. The absorption correction curves obtained this way are indicated in Fig. 20. In determining the efficiency of C_2 for the beta-spectrum, it was necessary to integrate the product of the theoretical allowed beta-spectrum of Hf^{181} (Feister (35)) and of the counter window transmission factor.

Consider first the coincidence rates obtained when the spectrometer was focused on α_{1L}. Instantaneous coincidences in this case were to be expected with the conversion electrons due to the transitions corresponding to γ_2, γ_3 and γ_4, and delayed coincidneces with the beta-spectrum. Experiments 1 and 2 show good agreement between observed and calculated values using two different absorber thicknesses between the source and C_2. Experiments 3, 4 and 5

Table IV

Electron - Electron Coincidence Measurements with Hf^{181}

Expt. No.	Spectral Component	N_c (c/m)	N_c/N_1 x 10^3	N_c/N_1 (Calc) x 10^3	Solid Angle for C_2 (%)	τ_c (μs)	Abs. (mg/cm^2)	Delay
1	α_{1L}	1.29 ± 0.11	2.61 ± 0.22	2.34	2	1.0	5 (mica)	0
2	α_{1L}	0.28 ± 0.04	0.63 ± 0.09	0.52	2	1.6	21.6 (Al)	0
3	α_{1L}	1.03 ± 0.13	2.38 ± 0.30	2.84	2	2.9	5 (mica)	0
4	α_{1L}	0.55 ± 0.11	1.28 ± 0.26	1.25	2	2.9	5 (mica)	6 μs C_2
5	α_{1L}	0.01 ± 0.12	0.02 ± 0.27	0	2	2.9	5 (mica)	6 μs C_1
6	α_{3K}	0.23 ± 0.06	2.13 ± 0.56	8.54	2	1.1	5 (mica)	0
7	α_{3K}	0.02 ± 0.04	0 ± 0.41	0.41	5	1.2	21.6 (Al)	0
8	α_{4K}	0.44 ± 0.04	6.4 ± 0.6	4.95	2	1.2	5 (mica)	0
9	α_{4K}	0.053 ± 0.019	0.8 ± 0.3	0.16	5	1.3	21.6 (Al)	0

Table IV (con'd)

Expt. No.	Spectral Component	N_c (c/m)	$N_c/N_1 \times 10^3$	N_c/N_1 (Calc) $\times 10^3$	Solid Angle for C_2 (%)[2]	τ_c (μs)	Abs (mg/cm^2)	Delay
10	β	0.087 ± 0.042	0.45 ± 0.22	0.34	2	1.5	5 (mica)	0
11	β	0.058 ± 0.025	0.35 ± 0.15	0.05	5	1.2	21.6 (Al)	0
12	β	0.148 ± 0.055	0.86 ± 0.32	0.67	2	2.8	5 (mica)	0
13	β	0.099 ± 0.057	0.60 ± 0.34	1.12	2	2.8	5 (mica)	6 μs C_1

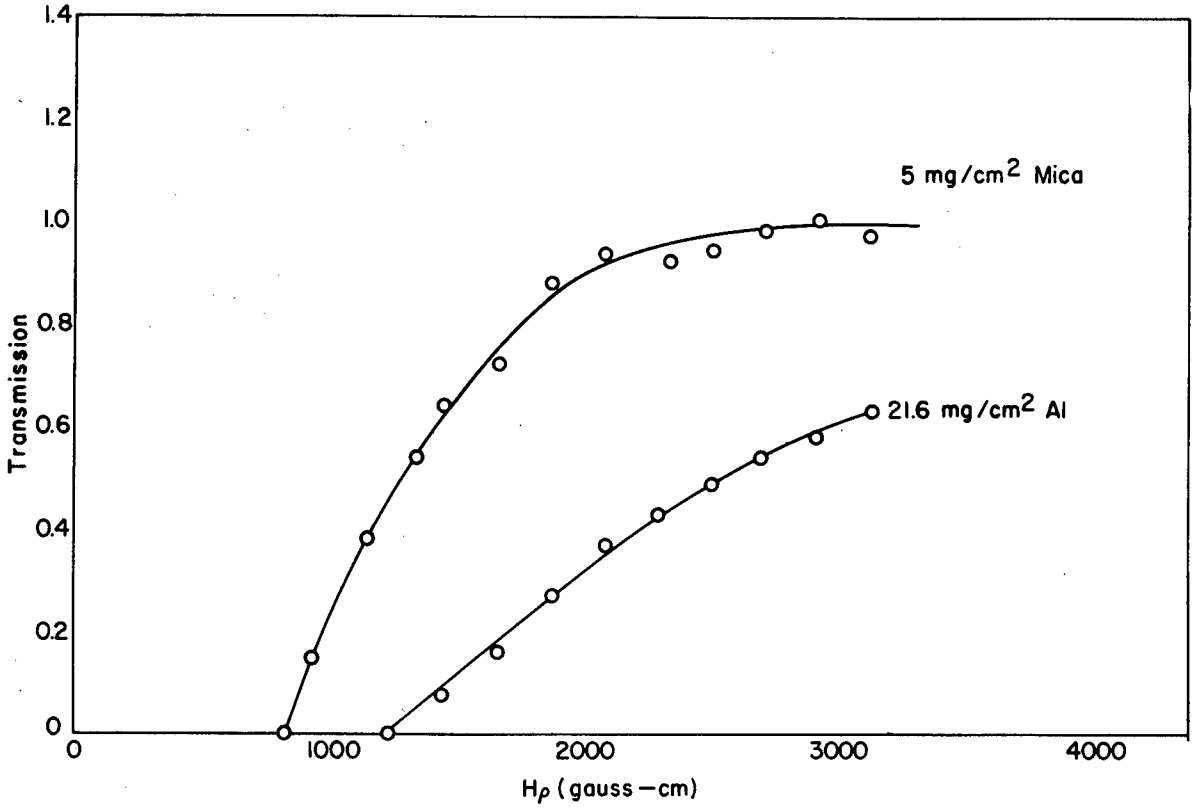

Fig. 20--Transmission of mica and aluminum films for electrons of different momenta.

indicate the results of introducing delays into each of the counter circuits. In experiment 4, in which a delay was introduced in the circuit of C_2, coincidences were to be expected between the beta-rays, and the conversion electrons represented by α_{1L}. it is seen that there is good agreement between the calculated and observed values. This rules out the possibility that the metastable state occurs after the transition γ_1. This conclusion is also verified by experiment 5, which indicated no delayed coincidences between γ_1 and any subsequent transitions.

In the case where the spectrometer was focused on α_{3K} or on α_{4K} it is seen from experiments 6-9 that the coincidence rates were reduced by a large factor when a 21.6 mg/cm^2 aluminum absorber (which is of a thickness approximately equal to the range of the conversion electrons corresponding to the transition γ_{1p}) was introduced between the source and C_2. This is in agreement with the decay scheme of Fig. 18, which indicates that γ_3 and γ_4 are in coincidence with γ_1.

In experiments 10-13, the spectrometer was focused on the beta-spectrum alone. Although the errors are large, an order of magnitude agreement with the decay scheme of Fig. 18 is indicated by these results.

Analysis of the coincidence data assuming the modification of Deutsch and Hedgran: Consider now the modification of the decay scheme of Hf^{181} proposed by Deutsch and Hedgran (52). These authors suggest that γ_3 is not included in this decay scheme, since they have found the relative intensities of γ_3 and γ_4 to differ in sources of different age. A slight increase with time in the ratio of γ_{3K} to γ_{4K} was also observed in the course of the present work. However, over a period of 140 days, this ratio increased by only a factor of 1.24 whereas an increase by a factor of 2 would be expected if these peaks were due to Hf^{175} and Hf^{181} respectively. Since the source was of a moderate thickness and was deposited somewhat loosely, it is not impossible that some change in the observed ratio α_{3K}/α_{4K} could be caused by movement of the source deposit with a corresponding change in the factor $S(\alpha)$ defined in section V. E.

If it is assumed that γ_3 is due to some process such as K capture in Hf^{175}, then a quantitative analysis of the coincidence data becomes particularly difficult since the unknown conversion probabilities may no longer be calculated on the basis of the decay scheme of Fig. 17. A

qualitative comparison may be made between experimental and calculated values by arbitrarily assuming γ_3 to have the same conversion coefficients and relative intensity as determined from the data of Chu and Wiedenbeck. Calculations may then be made for two different cases:

Case I: The beta- decay of Hf^{181} is followed by γ_1, γ_4 and γ_2 in cascade. The K capture process in Hf^{175} is followed by γ_3. This assumption is not consistent with the observed relative intensities of the transition corresponding to γ_2 and that corresponding to γ_4, but it will be useful to consider the results of a coincidence measurement to be expected with a decay scheme of this general type.

Case II: The beta-decay of Hf^{181} is followed by γ_1 and γ_4 in cascade. The K capture process in Hf^{175} is followed by γ_3 and γ_2 in cascade.

The coincidence rates calculated for Case I and Case II are compared in Table V with the experimental values and the values calculated on the basis of Fig. 17. Column 1 indicates the experiment code number, and column 2 indicates the spectral component on which the spectrometer was focused. Column 3 indicates the observed ratio N_c/N_1; and columns 4, 5 and 6 indicate respectively the calculated ratios N_c/N_1 assuming the decay scheme of Chu and Wiedenbeck, the decay scheme of Deutsch and Hedgran, Case I, and the decay scheme of Deutsch and Hedgran, Case II.

It is seen that the gamma-electron measurements do not serve to distinguish between any of the three alternatives. The gamma-electron absorption measurement (Fig. 19) is also consistent with any of these possibilities. The electron-electron measurements, with some exceptions, show fair agreement between either the decay scheme of Chu and Wiedenbeck or Case I of the decay scheme of Deutsch and Hedgran. The electron-electron experiment 7 in which the spectrometer was focused on the line α_{3K}, shows too few coincidences to agree with the decay scheme of Chu and Wiedenbeck and too many coincidences to agree with that of Deutsch and Hedgran. The effect of inserting an electron absorber between the source and C_2 indicates most of these coincidences to be due to soft electrons, which is qualitatively in agreement with the decay scheme of Chu and Wiedenbeck.

Table V

Summary of Coincidence Measurements with Hf^{181}

Expt. No.	Spectral Component	N_c/N_1 obs x 10^3	N_c/N_1 C and W x 10^3	N_c/N_1 D and H(I) x 10^3	N_c/N_1 D and H(II) x 10^3
		Gamma - electron measurements			
1	α_{1L}	0.795 ± 0.080	0.88	0.90	0.86
2	α_{3K}	0.83 ± 0.19	0.44	0.38	0.52
3	α_{4K}	0.71 ± 0.11	0.30	0.34	0.30
4	β	0.24 ± 0.08	0.10	0.10	0.10
5	α_{1L}	0.068 ± 0.085	0	0	0
6	β	0.089 ± 0.079	0.17	0.17	0.16
7	α_{1L}	0 ± 0.07	0	0	0
		Electron - electron measurements			
1	α_{1L}	2.61 ± 0.22	2.34	1.9	0.82
2	α_{1L}	0.63 ± 0.09	0.52	0.39	0.36
3	α_{1L}	2.38 ± 0.30	2.84	2.41	1.32
4	α_{1L}	1.28 ± 0.26	1.25	1.25	1.25
5	α_{1L}	0.02 ± 0.27	0	0	0

Table V (con'd)

Expt. No.	Spectral Component	N_c/N_1 obs x 10^3	N_c/N_1 C and W x 10^3	N_c/N_1 D and H(I) x 10^3	N_c/N_1 D and H(II) x 10^3
6	α_{3K}	2.13 ± 0.56	8.54	0.2	0.7
7	α_{3K}	0 ± 0.41	0.41	0.5	0.8
8	α_{4K}	6.4 ± 0.6	4.95	6.1	4.8
9	α_{4K}	0.8 ± 0.3	0.16	0.23	0.15
10	β	0.45 ± 0.22	0.34	0.33	0.27
11	β	0.35 ± 0.15	0.05	0.03	0.03
12	β	0.86 ± 0.32	0.67	0.61	0.51
13	β	0.60 ± 0.34	1.12	1.0	0.8

Summary: It may be concluded from the gamma-electron absorption measurement that γ_1 is in coincidence with γ_4. The gamma-electron measurements 1, 5 and 7, in which the spectrometer was focused on α_{1L} and delayed and non-delayed coincidences were sought, indicates that there are no delayed coincidences between γ_1 and any other gamma-ray. Thus, since γ_1 presumably originates in the metastable state, γ_1 must precede γ_4. The gamma-electron measurements 4 and 6, in which the spectrometer was focused on the beta-spectrum, indicate that the beta-spectrum is separated from γ_1 and γ_4 by the metastable state. The electron-electron measurements 1-5 and 10-13 are in reasonable agreement with these conclusions. Thus, the part of the decay scheme of Chu and Wiedenbeck which involves the beta-spectrum, γ_1 and γ_4 is verified by the measurements reported here.

These measurements do not serve to distinguish between the complete decay scheme of Chu and Wiedenbeck and the modification proposed by Deutsch and Hedgran. With a few discrepancies, for which no reasonable explanation has been found, both the electron-electron measurements and the gamma-electron measurements are in fair agreement with either alternative.

VII. LITERATURE CITED

1. Siegbahn, K. Untersuchungen über die Verwendung der magnetischen Linse für β - Spektroskopie. Arkiv för Mathematik, Astronomi och Fysik. 28A(no. 17): 1-27. 1942.

2. Deutsch, M., Elliott, L. G. and Evans, R. Theory, Design, and Applications of a Short Magnetic Lens Electron Spectrometer. Review of Scientific Instruments. 15:178-195. 1944.

3. Jensen, E. N. The Determination of Gamma Ray Energies with the Magnetic Lens Spectrometer. Atomic Energy Commission Document 2399. p. 1-70. 1947.

4. Witcher, C. M. An Electron Lens Type of Beta-Ray Spectrometer. Physical Review. 60:32-42. 1941.

5. Frankel, S. A Beta-Ray Spectrometer Design of Quadratic Resolution-Solid Angle Relationship. Physical Review. 73:804. 1948.

6. Keller, J. M., Koenigsberg, E. and Paskin, A. Ring Focus in a Thin Magnetic Lens Beta-Ray Spectrometer. Physical Review. 76: 454-455. 1949.

7. _____ Ring Focus in a Thin Magnetic-Lens Beta-Ray Spectrometer. To be published in the Review of Scientific Instruments.

8. Verster, N. F. Theory of a Magnetic Lens Type Beta Ray Spectrometer. Applied Scientific Research. B1(no. 5):363-378. 1950.

9. Mitchell, A. The Use of Coincidence Counting Methods in Determining Nuclear Disintegration Schemes. Reviews of Modern Physics. 20:296-304. 1948.

10. Dunworth, J. V. The Application of the Method of Coincidence Counting to Experiments in Nuclear Physics. Review of Scientific Instruments. 11:167-180. 1940.

11. Downing, J., Deutsch, M. and Roberts, A. Disintegration Scheme of the Yttrium Activity of 100-Day Half-Period. Physical Review. 60:470. 1941.

12. Roberts, A., Downing, J. and Deutsch, M. A Study of the Radiations from the Disintegration of Br^{82}. Physical Review. 60:544-550. 1941.

13. Downing, J., Deutsch, M. and Roberts, A. Disintegration Schemes of Radioactive Substances. III. I^{131}. Physical Review. 61:686-691. 1942.

14. Deutsch, M. and others. Disintegration Schemes of Radioactive Substances. IV. Fe^{59}. Physical Review. 62:3-7. 1942.

15. Roberts, A. and others. Disintegration Schemes of Radioactive Substances. V. I^{130}. Physical Review. 64:268-275. 1943.

16. Elliott, L. G. and Deutsch, M. Disintegration Schemes of Radioactive Substances. VI. Mn^{56} and Co^{56}. Physical Review. 64:321-331. 1943.

17. Norling, F. The Coincidence Method and Its Applications to Disintegration Problems. Arkiv för Mathematik, Astronomi och Fysik. 27A(no. 27):1-95. 1941.

18. Siegbahn, K. and Johansson, A. Coincidence-Spectrometry for Disintegraion Problems. Arkiv för Mathematik, Astronomi och Fysik. 34A(no. 10):1-19. 1946.

19. Feather, N., Kyles, J. and Pringle, R. Investigations Using a Permanent-magnet Double β-Ray Spectrograph with Coincidence Counting - I. Experiments with Thorium Active Deposit. Proceedings of the Physical Society (London). 61:466-478. 1948.

20. Persico, E. Optimum Conditions for a Beta-Ray Solenoid Spectrometer. Physical Review. 73:1475-1476. 1948.

21. Slatis, H. and Siegbahn, K. A New Type of Focusing in a Magnetic Lens Field. Physical Review. 75:1955. 1949.

22. Persico, E. A Theory of the Solenoid Beta-Ray Spectrometer. Review of Scientific Instruments. 20:191-196. 1949.

23. Du Mond, J. W. M. Conditions for Optimum Luminosity and Energy Resolution in an Axial β-Ray Spectrometer. Review of Scientific Instruments. 20:160-169. 1949.

24. Heitler, W. The Quantum Theory of Radiation. 2d ed. London, Oxford University Press. 1944.

25. Hornyak, W. F., Lauritsen, T. and Rasmussen, V. K. Gamma-Ray Measurements with a Magnetic Lens Spectrometer. Physical Review 76:731-739. 1949.

26. Jensen, E. N., Laslett, L. J. and Pratt, W. W. A Revaluation of the Gamma-Radiations from Co^{60} and Zn^{65}. Physical Review. 76:430. 1949.

27. Mandeville, C. E. and Scherb, M. V. Nuclear Disintegration Schemes and the Coincidence Method. Nucleonics. 3(no. 4):2-12. 1948.

28. Korff, S. A. Electron and Nuclear Counters. New York, D. Van Nostrand Co. 1946.

29. Deutsch, M., Elliott, L. G. and Roberts, A. Disintegration Schemes of Radioactive Substances VIII. Co^{60}. Physical Review. 68:193-197. 1945.

30. von Droste, G. F. "Über die Anzahl der Ausschläge eines Zählrohres bei Bestrahlung mit γ-Strahlen verschiedener Wellenlänge." Zeitschrift für Physik. 100:529-533. 1936.

31. Worthing, A. G. and Geffner, J. Treatment of Experimental Data. New York. John Wiley and Sons. 1943.

32. Rutherford, E., Chadwick, J. and Ellis, C. D. Radiations from Radioactive Substances. Cambridge, University Press. 1930.

33. Moak, C. D. Construction Features of a Circuit for Coincidence Measurements and Applications of the Circuit to Nuclear Problems. Manhattan District Declassified Document 1010. 1945.

34. Gallagher, J., Higinbotham, W. A. and Sands, M. The Model 200 Pulse Counter. Manhattan District Declassified Document 773. 1946.

35. Feister, I. Numerical Evaluation of the Fermi Beta-Distribution Function. Physical Review. 78:375-377. 1950.

36. Handbook of Chemistry and Physics. 25th ed. Cleveland, Chemical Rubber Publishing Co. 1941.

37. Hulme, H. R. and others. The Photoelectric Absorption of γ-Rays in Heavy Elements. Proceedings of the Royal Society of London. Series A. 149:131-151. 1935.

38. Compton, A. H. and Allison, S. K. X-Rays in Theory and Experiment. 2nd ed. New York, D. Van Nostrand Co. 1935.

39. Martin, D. G. E. and Richardson, H. O. W. The Nuclear β-Spectra of Thorium B $\rightarrow$ C and C $\rightarrow$ C' and the Intensities of Some β-Ray Lines of Thorium (B + C + C''). Proceedings of the Royal Society of London. Series A. 195:287-300. 1948.

40. Rasetti, F. Elements of Nuclear Physics. New York, Prentice-Hall. 1936.

41. Chu, K. Y. and Wiedenbeck, M. L. The Radiations from Hf^{181}. Physical Review. 75:226-231. 1949.

42. Beneš, J. and others. Decay Scheme of Hf^{181}. Nature. 162:261-262. 1948.

43. Mandeville, C. E., Scherb, M. V. and Keighton, W. B. Radiations from Cd^{115}, In^{115}, and Hf^{181}. Physical Review. 75:221-226. 1949.

44. Lundby, A. The Decay Scheme of Hf^{181}. Physical Review. 76:1809-1811. 1949.

45. Jensen, E. N. Radiations from Hf^{181}. Physical Review 76:958-961. 1949.

46. Bunyan, D. E. and others. The Delayed Coincidence Method in the Study of Radioactivity, with Applications to Isomerism in ^{181}Ta. Proceedings of the Physical Society (London). 61:300-306. 1948.

47. Voigt, A. F. and Thamer, B. J. Studies on the Radiation from Hf^{181}. Atomic Energy Commission Document 2083. 1948.

48. Cork, J. M. and others. Radioactivity in Hf. Physical Review. 78:299. 1950.

49. McGowan, F. K. Short Lived Isomers. Oak Ridge National Laboratory Report 694. p. 19-23. 1950.

50. De Benedetti, S. and McGowan, F. K. Short-Lived Isomers of Nuclei. Physical Review. 74:728-735. 1948.

51. Chang, C. S. W. and Falkoff, D. L. On the Continuous Gamma-Radiation Accompanying the Beta-Decay of Nuclei. Physical Review. 76:365-371. 1949.

52. Deutsch, M. and Hedgran, A. Radioactivity of Hf^{181}. Physical Review. 79:400-401. 1950.

VIII. ACKNOWLEDGEMENTS

It is a pleasure to express sincere appreciation to Dr. L. J. Laslett, of the Physics Department, for suggesting the problems and for many valuable suggestions during the progress of the work. The author is also greatly indebted to Dr. E. N. Jensen and Dr. J. M. Keller, also of the Physics Department, for many helpful discussions concerning the theory and operation of the spectrometer. Expressions of appreciation are also due to Dr. A. Voigt, Dr. D. S. Martin, Mr. D. M. Hiller and Mr. E. H. Dewell, of the Chemistry Department, for preparation of radioactive sources for the spectrometer; to Mr. F. I. Boley, Mr. E. Koenigsberg, Mr. A. Paskin, Mr. R. T. Nichols and Mr. J. Clement, of the Physics Department, for assistance with the work on Ring Focusing; to Mr. R. O. Lane, of the Physics Department, for assistance with the taking and analyzing of data and with the construction of the equipment; to Mr. I. Coleman and the staff of the Iowa State College Instrument Shop for solution of many of the mechanical problems; to Mr. E. R. Rathbun, of the Physics Department, for design and construction of the Geiger counters used; and to Mr. W. J. Mueller and the staff of the Electronics Shop for the design and construction of much of the electronic equipment. Finally, the author would like to express his appreciation to Mrs. Margaret Kirwin for valuable assistance with the preparation of the manuscript.

END OF DOCUMENT